A COMPUTATIONAL APPROACH TO SMOOTHEN THE ABRUPT STIFFNESS VARIATION ALONG RAILWAY TRANSITIONS

Muhammad Babar Sajjad

PhD Candidate, S.M.ASCE

Transport Research Centre, School of Civil and Environmental Engineering, University of Technology Sydney, Ultimo, Sydney, Australia

Buddhima Indraratna*

Distinguished Professor, and Director, PhD

FTSE, FIEAust, FASCE, FGS, FAusIMM, FIESL, DIC, CEng, CPEng

Transport Research Centre, School of Civil and Environmental Engineering, University of Technology Sydney, Ultimo, Sydney, Australia

Trung Ngo

Senior lecturer, PhD, CPEng, M.ASCE

Transport Research Centre, School of Civil and Environmental Engineering, University of Technology Sydney, Ultimo, Sydney Australia

Richard Kelly, PhD

Chief Technical Principal, SMEC

Brisbane, Queensland, Australia

Cholachat Rujikiatkamjorn

Professor, PhD, CPEng, M.ASCE

Transport Research Centre, School of Civil and Environmental Engineering, University of Technology Sydney, Ultimo, Sydney, Australia

Submitted to: ASCE - Journal of Geotechnical & Geoenvironmental Engineering

*Corresponding author: Buddhima Indraratna (buddhima.indraratna@uts.edu.au)

A Computational Approach to Smoothen the Abrupt Stiffness Variation along Railway Transitions

Muhammad Babar Sajjad[a], Buddhima Indraratna[b], Trung Ngo[c], Richard Kelly[d], Cholachat Rujikiatkamjorn[e]

[a]PhD student, School of Civil and Environmental Engineering, University of Technology Sydney, Ultimo, Sydney, Australia; Email: MuhammadBabar.Sajjad@student.uts.edu.au
[b]Distinguished Professor of Civil Engineering and Director of Transport Research Centre, University of Technology Sydney, Ultimo, Australia; Founding Director, ARC Industrial Transformation Training Centre for Advanced Technologies in Rail Track Infrastructure (ITTC-Rail), University of Wollongong, Australia; Email: buddhima.indraratna@uts.edu.au
[c]Senior lecturer, Transport Research Centre, School of Civil and Environmental Engineering, University of Technology Sydney, Ultimo, Australia; Email: Trung.Ngo@uts.edu.au
[d]Chief Technical Principal at SMEC, Brisbane, Queensland, Australia; Email: DrRichard.Kelly@smec.com
[e]Professor, School of Civil and Environmental Engineering, University of Technology Sydney, Ultimo, NSW 2007, Australia; Email: Cholachat.Rujikiatkamjorn@uts.edu.au

Abstract: This paper presents a novel approach to smoothen the abrupt stiffness variation along railway transitions and provides step-by-step design of a multi-step transition zone comprising adjoining segments with changing stiffness values. The influence of stiffness on track dynamic response applied to transition zones is investigated analytically, considering a beam on elastic foundation. Vertical track displacements for varying stiffness values under different combinations of axle loads and speeds are calculated analytically and numerically, and they are found to be in good agreement. The results indicate that the stiffer tracks undergo lesser settlements compared to those having a smaller stiffness. The effect of abrupt stiffness variation at transition sections is analysed under four-carriage loading causing considerable differential settlement, which is further exacerbated by increased train speeds. A mathematical process is introduced to determine the optimum stiffness of each segment to ensure a gradual change in stiffness while minimising the corresponding differential settlement. The proposed methodology is further validated through the Finite Element Modelling approach and worked-out examples epitomizing the effects of stiffness variation along the number of transition steps. From a practical perspective, this study provides a significant extension for design rejuvenation of transition zones by minimising the differential settlement at any two consecutive transition segments.

Introduction

Abrupt changes in stiffness at track transitions (e.g. bridge and tunnels approaches and crossings) have been mostly considered the dominant source of numerous track dynamic concerns, including differential track settlements, severe vibrations and instability (Kerr et al. 1993, Frohling et al. 1996, Lundqvist et al. 2005, Namura et al. 2007, Mishra et al. 2014). The overall (global) stiffness of the rail track can vary considerably depending on its structural components and subgrade characteristics (Powrie et al. 2016). For example, a significant stiffness variation can be expected when a rail track with a soft natural subgrade (e.g. conventional ballasted track on soft and weak subgrade) changes to a stiffer track (e.g. slab track or concrete bridge deck) or vice versa. Consequently, a large differential settlement occurs at track transition, leading to accelerated track degradation, enhanced passenger discomfort, and higher maintenance costs (Zarembski et al. 2003, Pita et al. 2004, Li et al. 2005, López-Pita et al. 2007, Dahlberg 2010, Choi 2013, Tutumluer et al. 2013, Zhou et al. 2020, Luo et al. 2021). Therefore, a transition zone with smooth and gradual stiffness variation needs to be provided at these locations to alleviate the problems linked to such structural discontinuities (Indraratna et al. 2011, Zuada Coelho 2011, Sañudo et al. 2016, Aggestam et al. 2019).

The research into track dynamics involves the study of induced vibrations of track and vehicle in all directions under the effect of moving loads (Van Dalen 2006, Zhai et al. 2013, Kouroussis et al. 2014, Real et al. 2016). It considers various components of the track structure react to the applied loads according to their inherent frequencies and finds that a significant amplification of track vibrations could occur when these frequencies reach their natural frequencies (i.e. resonant effect) (Esveld 2001). Increased train speed can lead to amplified dynamic vibrations on track structure due to propagation of surface waves and bending waves in track (Kouroussis et al. 2014). For conventional tracks, these vibrations become exacerbated, especially when the train speed reaches some critical velocities; causing strong vibrations to track structures and noise to surrounding buildings (Dimitrovová et al. 2009, Galvín et al. 2010, Zhai et al. 2013).

There are various factors that are responsible for such vibrations including: train speed, dynamic locomotive power, track irregularity, hanging sleepers, rail welding slag and joints, and wheel irregularities (Le Pen et al. 2014, Lei 2017, Abadi et al. 2019). Track transition is also one of the types of track irregularities that creates an abrupt change in track structural properties (i.e. stiffness) both in time and space (Indraratna et al. 2019). At such a location, the vibrations become further enlarged, causing increased dynamic loading and differential settlements leading to accelerated track degradation (Plotkin et al. 2008, Berggren et al. 2010, Woodward et al. 2012, Huang et al. 2013, Ramos et al. 2020). The effects of track transition on track acceleration, rail deflection and the dynamic load are summarised in Fig. 1, which has been reproduced from the data given in Esmaeili et al. (2018). This figure shows the track response to a moving load at a location where the track changes suddenly from soft to stiff track, and a sharp change in the track response for the track acceleration, rail deflection and the dynamic loading can be noted at this transition.

Major problems related to railway transitions, such as enhanced dynamic load, differential settlements and accelerated track degradation are highly interconnected with each other, especially when moving trains with faster speeds and increased axle loads are involved (Frohling et al. 1996, Gallego Giner et al. 2009, Lei et al. 2010, Mishra et al. 2014, Shan et al. 2020). The cycle of these problems and their causes and effects are illustrated in Fig. 2. A comparison of a sudden increase in vertical displacement (Zhai et al. 2000, Sañudo et al. 2016, Heydari-Noghabi et al. 2017, 2018), and enhanced dynamic loads (Zhai et al. 2000, Nicks 2009, Lei et al. 2010, Wang et al. 2017) for various track transitions is also presented in Fig. 2. It can be noted that abrupt change in track structure, from stiff to soft or soft to stiff, causes a sudden increase in vertical displacement that results in the differential settlement at these locations. The maximum differential settlement based on the corresponding transient settlements, caused by the train loading, includes both the dynamic (elastic, hence recoverable) and the permanent (residual) differential settlement, hence the accumulated (total) vertical displacement. Granular soil types including ballast shall sustain a cumulative residual (permanent) settlement attributed to previous train passes, as well as any sleeper-ballast gap formed due to ballast breakage, which contributes to increased total differential settlement during the train passage (Mishra et al. 2017). Fig. 2 also shows high impact forces at wheel/rail contact indicating the enhanced dynamic loadings at these junctions. This illustration further shows how the dynamic load and differential settlement are interdependent at a track transition, with every spike in one variable causing a corresponding rise in the other in a cyclical fashion, and how they affect track degradation. Further details of track transition-related problems under the dynamic effect of moving trains can be found in Indraratna et al. (2019).

Although there have been several mitigation measures, utilised to minimise the track transition problems, and a few computational processes in relation to transition zones as reported by Indraratna et al. (2019), but they have not provided any rigorous guidelines or comprehensive procedures for design. The literature in this field is lacking in respect to any specific fundamental approach that can be used in the design of track transitions incorporating the actual ground conditions, especially to cater for long and heavy haul freight in Australia. Therefore, a precise and economical design of transition zones remains a challenge for rail practising engineers. To the knowledge of the authors, there have been no other studies focused particularly primarily on the effects of abrupt stiffness variations and a fundamental optimization procedure to minimize the differential settlements. Indeed, from the outset, this has been the main reason for the motivation of this study.

This paper presents a novel analytical approach that can be used in the design of rail track transition zones. This fundamental approach provides a step-by-step design of a multi-step transition zone considering the abrupt change of stiffness at any transition. It determines the optimum stiffness of each segment at a transition zone to ensure a smooth and gradual change in stiffness values along the track. The optimum stiffness of each segment is then utilised as input stiffness parameters for a layered track that is simulated using the Finite Element Method (FEM) in ABAQUS to capture the response of different track elements (e.g. ballast, sub-ballast and subgrade). In this regard, various factors associated with track transition are discussed first to highlight the importance of the transition zone. An analytical model is developed for a rail track considering a beam on elastic foundations (BOEF) subjected to various loading conditions (single, multiple and moving axle loads) to investigate the effect of track stiffness on track settlements.

A beam on springs model is then simulated, to verify the analytical model. This model is further developed into 2D FEM layered models for conventional ballast track considering:(i) no transition, (ii) one-step transition and (iii) multi-step transition. These models consider varied values of stiffness to simulate the moving wheel load on the layered track, where they are determined on the basis of the analytical approach. A proposed methodology for the novel approach of multi-step transition with examples for one-step and multi-step transition is discussed, followed by practical design guidelines, a flow chart, and two worked-out examples.

Analytical Modelling of Rail Tracks

In this section, an analytical model is proposed to investigate the effect of track stiffness on track dynamic response under train loadings as there have been limited studies to consider stiffness variation at track transition.

Beam on Elastic Foundation (BOEF) Model

The Euler-Bernoulli beam on elastic foundation theory has been extensively used to model railway tracks and transitions (Esveld 2001, Li et al. 2005, Mishra et al. 2014, Paixão et al. 2018) and it is adopted in this study to investigate the stiffness effect on track dynamic responses under multiple loadings. Following this approach, a continuous beam resting on an elastic foundation can be considered as a rail track structure to develop the corresponding load-deformation equation. In this study, a rail track is modelled by considering a steel beam with the modulus of elasticity (E), the moment of inertia (I), and mass per unit length (m), resting on a foundation with stiffness (k), and damping (c), as shown in Fig. 3(a). The term "foundation stiffness" or "track equivalent stiffness (k)" is adopted in this study in accordance with some previous studies, e.g. Lei (2017) and Priest et al.

(2009). This foundation stiffness represents the original definition of stiffness magnitude, relating the line load amplitude to the corresponding vertical displacement, with the units of MN/m/m or MN/m^2. The differential equation for the track system can be described as introduced by several authors (Kenney 1954, Esveld 2001, Zhang et al. 2017):

$$EI\frac{\partial^4 w}{\partial x^4} + m\frac{\partial^2 w}{\partial x^2} + c\frac{\partial w}{\partial x} + kw = -P\delta(x - vt) \tag{1}$$

where, w represents the vertical displacement (i.e. settlement) of rail at point x, at any time t, under a wheel load P, moving at speed, v. A vertical displacement of the rail for an undamped case can be derived as:

$$w = e^{\beta x}(C_1 cos\beta x + C_2 sin\beta x) + e^{-\beta x}(C_3 cos\beta x + C_4 sin\beta x) \tag{2}$$

where,

$$\beta = \sqrt[4]{\frac{k}{4EI}} \tag{3}$$

and C_1 to C_4 are constants that can be found by taking a physical example of an infinite beam with concentrated midpoint loading as P resting on an elastic foundation.

To ensure a finite deflection for this beam, the following boundary conditions must satisfy:

(i) at $x = \infty$: $C_1 = C_2 = 0$

$$w = e^{-\beta x}(C_3 cos\beta x + C_4 sin\beta x) \tag{4}$$

(ii): at $x = 0$, the slope of the deflection curve should be zero (i.e., for the symmetric shape of the deflected beam): $\frac{dw}{dx} = 0$

$$\frac{dw}{dx} = e^{-\beta x}(C_3 cos\beta x + C_4 sin\beta x) + e^{-\beta x}(\beta)(C_3 cos\beta x + C_4 sin\beta x) = 0 \tag{5}$$

which gives: $C_3 = C_4 = C$

The symmetric deflected shape indicates that the track stiffness remains constant along the track, whereas, while it varies spatially, in case of track transition. Therefore, at the junction of two consecutive segments, symmetric boundary conditions were assumed for the analytical solution. In this approach, the analytical solution calculates the maximum settlement for each segment to provide an assessment of the differential settlement at the track transition. Although the analysis assumes an infinite rail length (also conforms to plane strain), the symmetric assumption has a minimal impact on the evaluation of the spatial variability of stiffness, which is more a dependent on the subgrade conditions (Selig et al. 1994).

The solution for the rail deflection becomes:

$$w = Ce^{-\beta x}(cos\beta x + sin\beta x) \tag{6}$$

Considering the symmetry of the deflected shape, the loading condition should satisfy:

$$P = 2\int_{0}^{\infty} kCe^{-\beta x}(cos\beta x + sin\beta x)dx \tag{7}$$

Integrating by parts gives: $C = \frac{P\beta}{2k}$

Substituting C to Equation (5) gives:

$$w(x) = \frac{P\beta}{2k}e^{-\beta x}(cos\beta x + sin\beta x) \tag{8}$$

Numerical Modelling of Rail Tracks

Beam on Springs Model

In this study, the development of a complex finite element model of the rail track transition zone was carried out in a systematic manner, starting from a simple model and then gradually increasing its sophistication to predict the settlement under train loading. Initially, a beam on springs model was developed under static general conditions, using Finite Element Modelling software ABAQUS, to verify the analytical modelling technique. In this model a steel beam of flexural rigidity, EI is considered to be connected to the ground with equally spaced springs of specific stiffness S, as shown in Fig. 3(b). The material properties and cross-sectional profile of the steel beam, as well as the spring stiffness and spacing, have been selected to align with the material parameters used for analytical modelling for varying stiffness values (Table 1). The total length of the model has been considered as 10m to avoid any boundary effect for single midpoint loading, P (Fig. 3b). This straightforward and relatively simple numerical model can be used to examine how track stiffness affects track settlement under train loadings. The model is analysed for various stiffness values and loadings and the results are compared with those that are calculated through analytical modelling as provided in the next sections. This numerical model provided similar results as the analytical model considering the BOEF concept (beam on elastic foundation) as shown in Fig. 3(a).

2D FEM Layered Model

The beam on springs model was further upgraded to a two dimensional (2D) layered model consisting of rail, ballast, sub-ballast and subgrade layers to simulate the conventional ballast track. To investigate the effect of train wheel load, a 2D plain strain model, with a total length and height of 9.86m and 5.68m respectively, was developed using FEM software ABAQUS as shown in Fig. 3(c). The steel rail is modelled as a modified rectangular section, (width=50mm, height=194mm), for a standard UIC60 profile with 60kg/m as the unit mass (Shahraki et al. 2015). There are 17 reinforced concrete sleepers, each measuring 0.26 metres in width and 0.23 metres in height, with a 0.6-meter space between them (Nimbalkar et al. 2016). Ballast and sub-ballast layers have been kept at thicknesses of 300 mm and 150 mm, respectively, and are situated on top of a homogenous subgrade that is 5 metres thick.

Due to the anticipated non-yielding behaviour, the steel rail and concrete sleepers are modelled as linear-elastic materials. However, to accurately represent the damping and nonlinear behaviour of track substructure, the ballast, sub-ballast and subgrade are modelled as viscoelastic materials with the inclusion of damping behaviour (Nimbalkar et al. 2012, Lamprea-Pineda et al. 2021). In this regard, the Rayleigh viscous damping technique is utilised, where the global damping matrix (C) is related to the mass matrix (M), and stiffness matrix (K), through Rayleigh damping coefficients; α

and β, as shown below (Chumyen et al. 2022).

$$C = \alpha M + \beta K \tag{9}$$

The geometry and model input parameters for the substructural elements used in the current FE analysis are obtained from Indraratna et al. (2018), which were derived from extensive laboratory testing carried out in New South Wales, Australia (Indraratna et al. 2011). The summary of the mechanical parameters for each component of the track models used for this investigation can be found in Table 1.

Track geometry, boundary conditions, element size, and dynamic calculation time-step for this model have been established properly to ensure an adequate level of accuracy for the track dynamic analysis. The model represents a vertical cross-section through the centreline of one of the rails along the track, for a conventional ballast track. Vertical displacement has been allowed on both the vertical boundaries of the model, whereas, the encastre boundary condition has been applied at the bottom of the model to constrain all displacements and rotations at a node to zero, meaning U1 = U2 = U3 = UR1 = UR2 = UR3 = 0. It is noted that the sides and base of the model do not transmit waves, however, the wave reflection during the current analysis is not an issue due to the applied static loadings. The maximum element sizes for sub-ballast, ballast, and subgrade layers have been kept as 0.075m, 0.13m, and 0.1-1m, respectively. Hence, the discretised mesh grid has 2234 nodes and 1834 hourglass-controlled quadrilateral plain strain elements (element type: CPE4R), including 100 linear line elements for the steel rail. In order to improve the analysis accuracy, the node continuity at the interface is well maintained between all the layers. Additionally, surface-to-surface contact was established between various layers of the track model using a penalty method to ensure the accurate transmission of normal and shear stresses at the interface (Hibbitt et al. 2014).

Model Validation

Both the numerical models; the beam on spring and the 2D layered, are validated with the analytical model and field data reported by Read et al. (2006), by comparing the maximum settlement under wheel loads for various track stiffness. In this regard, the analytic response was obtained by solving Equation (8) for stiffness values, k = 9 MN/m/m and 64 MN/m/m, under wheel loads, P = 7 tonnes. The track stiffness values, and the wheel load are adopted in accordance with the data reported by Read et al. (2006) for model validation under similar loading conditions. Beam on spring model is then solved numerically for the same loads considering a steel beam resting on equally spaced springs with stiffness values of 9 MN/m and 64 MN/m placed at the one-meter centre to centre distance. The wheel load is applied at the centre of the model to determine the maximum settlement under the applied loading. The deformation contour showing the maximum settlement and the deformed shape of this FE model with 9 MN/m/m stiffness springs, is given in Fig. 4(a), which indicates a maximum settlement of 2.9 mm under 7 tonnes wheel loading which is in good agreement with the one obtained analytically.

Likewise, the 2D layered FEM model is solved numerically for the same loading conditions where an equivalent track stiffness (k) for this model is used to match its values with the analytical model. The equivalent track stiffness is a combination of stiffness from various track components, that contribute in a series form, for example in the case of a layered ballast track, it can be calculated as given below (Powrie et al. 2016):

$$\frac{1}{k_b} = \frac{1}{k_{railpad}} + \frac{1}{k_{sleeper}} + \frac{1}{k_{ballast}} + \frac{1}{k_{Sub-ballast}} + \frac{1}{k_{subgrade}} \tag{10}$$

The stiffness of rail pads and sleepers is primarily determined by the resilience and stiffness of their elastomeric components. As a result, equivalent stiffness of rail fastening system is more uniform and easier to predict compared to the track substructural components (e.g. ballast, sub-ballast, subgrade). However, the stiffness of track substructure can be related to its fundamental properties; the Poisson ratio, Young's modulus, and the thickness of individual layers as introduced by Lei (2017), as below:

$$k = \frac{0.65E_s}{1 - v_s} \sqrt[12]{\frac{E_s B^4}{EI}} \tag{11}$$

where, k represents the track foundation stiffness in MN/m per meter length (MN/m/m); E_s and v_s represent foundation elastic modulus in MN/m^2 and Poisson's ratio, respectively. B is the sleeper length, and EI is the flexural modulus of the rail in MN m^2.

For a three layered model, the foundation elasticity modulus, E_s can be calculated as per Zhang et al. (1998), that can be reproduced as below:

$$E_s = \left\{ \frac{h_1 \sqrt[3]{E_1} + h_2 \sqrt[3]{E_2} + h_3 \sqrt[3]{E_3}}{h_1 + h_2 + h_3} \right\}^3 \tag{12}$$

where, E_1, E_2, E_3 and h_1, h_2, h_3 are the modulus of elasticity in MN/m^2 and thickness of model layers from top to bottom.

This indicates that any change in the material properties of the track components will result in the corresponding change in its overall stiffness. In this model, the change in overall stiffness values has been achieved by changing the E values of ballast, sub-ballast and subgrade where the other material properties are kept the same (as given in Table 1) for all cases. Hence, to achieve the overall stiffness of 9 MN/m/m and 64 MN/m/m, the E values of ballast, sub-ballast and subgrade are calculated using Equations (10), (11), & (12) as given in Table 2. The wheel load is applied at the centre of the model as a point load to determine the maximum settlement under the applied loading. The deformation contour showing the maximum settlement and the deformed shape of this FE model with overall stiffness of 9 MN/m/m, is given in Fig. 4(b). It is seen that the maximum settlement of 2.9 mm is predicted under 7 tonnes wheel loading, which is almost the same as the analytical solution and beam on springs model.

The comparison of vertical displacements of tracks for these models is presented in Fig. 4(c). To validate the FEM model, predicted settlements were compared with field data reported by Read et al. (2006). As seen in this figure, both studies show a comparable maximum settlement and deformation pattern under similar loading conditions, albeit some discrepancy in the deformation pattern obtained from 2D FE modelling (layered) and from the authors' analytical model. This could be attributed to the differences in modelling assumptions, especially where the analytical model assumes the loads being supported by a series of vertical springs with zero deformation for nearby soil elements, while the FEM numerical model distributes the applied loads in both transverse and horizontal directions. Additionally, the non-linearity of layered materials and the damping values may result in a more spatial distribution of deformation (Walker et al. 2018). However, it can be noted that the maximum displacement, under a given wheel load P, for all the three models (analytical, beam on spring, 2D layered) is almost similar. For example, the maximum settlement under 7 tonnes wheel loading for all three models having a track stiffness value of 9 MN/m/m is about 2.9mm which is identical for all. In case of track transition, the maximum settlement calculated for each sides segment provides an assessment of the differential settlement, which is the main design criterion. Hence, the 2D layered model can be used to study the dynamic response of ballasted tracks under various loading conditions. Fig. 4(c) also shows an increase in vertical displacement with the decrease in track stiffness, a detailed discussion of this phenomenon is given in the next section.

Effect of Track Stiffness on Track Settlement

Effect of Track Stiffness on Track Settlement under single-wheel loading

In order to investigate the effect of track stiffness in terms of track settlement under train loading, Equation (8) is solved for various stiffnesses under a given wheel load of P = 7.5-17.5 tonnes (representing 15-35 tonne axle loads). The stiffness values (k = 5-80 MN/m/m) have been adopted in this study based on past studies (Dahlberg 2010, Powrie et al. 2016, Sung et al. 2020). In this article, k represents the overall track stiffness, demonstrating the load required to produce a unit track deflection and can be determined from field measurements either by measuring rail/sleeper deflection under actual train passing or by falling weight techniques (Powrie et al. 2016). The loading range has been selected to incorporate typical Australian heavy-haul railways that correspond to 35-tonne axle loading (i.e. P = 17.5 tonnes). Additionally, the track stiffness effect was also analysed numerically using the beam on spring model under the above loading for various spring stiffness values (i.e. k = 5-80 MN/m/m).

The results obtained from analytical and numerical modelling are presented in Fig. 5, which demonstrate exactly similar observations for both modelling approaches. The results indicate a decrease in vertical displacement (w) with an increase in track stiffness (k) for a given applied load (P), as expected (Choudhury et al. 2008). For example, Fig. 5a shows the decrease in maximum track settlement, w_{max} under 15-tonne axle load, from 4.9mm to just 0.6mm for an increase in track stiffness from k=5MN/m/m to 80MN/m/m. This affirms that the stiffer tracks undergo lesser settlements than the tracks having a smaller stiffness. It can also be noted that the settlement increases with the increase in applied load, indicating the higher differential settlements at track transitions due to load amplification. A maximum track settlement (w_{max}) for the case of 15-tonne axle load and k =5MN/m/m (Fig. 5a) is predicted as about w_{max}=4.9mm, compared to w_{max}=11.5mm for similar track stiffness subjected to 35-tonne axle load (Fig. 5d). Hence, it can be concluded that higher differential settlements occurring at the track transitions can be amplified by sudden stiffness variation and train loading.

Effect of Track Stiffness on Track Settlement for Multiple and Moving Train Loadings

The effect of multiple loading can be considered by modifying Equation (8) for multiple loadings, introduced by (Esveld 2001):

$$w(x) = \sum_{p=1}^{N} \frac{P\beta}{2k} e^{-\beta(x-d_p)}\left(\cos\left(\beta\left(x-d_p\right)\right) + \sin\left(\beta\left(x-d_p\right)\right)\right) \tag{13}$$

where, $w(x)$ = Maximum track settlement at any point x under the effect of multiple loadings, N = Total number of load points for the whole train; P = Wheel load; and d_p = Distance of a certain load point from point x.

In order to investigate the effect of multiple loading, Equation (13) was solved analytically for a four-carriage loading (16 wheels) as shown in Fig. 6(a). In this study, the values of D_1, D_2 and D_3 have been considered 2.5m, 12m and 4m, respectively (Hendry 2007). The equation was solved for three different track stiffnesses (5MN/m/m, 10MN/m/m, and 40MN/m/m), under P=10-tonne. A similar problem was also solved numerically by extending the length of 2D FEM layered model (as discussed above) to 120m, simulating a four-carriage train loading and using the material properties as given in Table 1 and Table 2. The vertical displacements of the rail under the effect of multiple (16 wheels) loadings obtained through analytical and numerical modelling are presented in Fig. 6(b). A reasonable agreement is found for maximum displacements under combined loading obtained from both analytical and numerical modelling approaches. Furthermore, comparing Fig. 5(b) and Fig. 6(b), it can be noted that the maximum track settlement (w_{max}) for k =5MN/m/m under 10-tonne single wheel loading (Fig. 5b) increases from 6.5mm to 8mm when considering the effect of multiple train loadings (Fig. 6b). A considerable increase in track settlement under each wheel load can be observed, demonstrating the pronounced effect of multiple wheel loading.

The effect of moving train with speed v, at any point x along the track with respect to time t, can be calculated using Equation (14):

$$w(x,t) = \sum_{p=1}^{N} \frac{P_d \beta}{2k} e^{-\beta(vt-d_p)} \left(\cos\left(\beta\left(vt - d_p\right)\right) + \sin\left(\beta\left(vt - d_p\right)\right)\right) \tag{14}$$

where, $w(x,t)$ = Maximum track settlement at point x with respect to time t, under the effect of multiple loadings, N = Total number of load points; P_d = Dynamic wheel load; d_p = Distance of a certain load point from point x; and v is the speed of the moving train.

The dynamic behaviour of tracks is captured in terms of increased deformations with increased speeds, as a function of the dynamic amplification factor (DAF). DAF determines the quasi-dynamic stress due to moving loads and incorporates the train speed, sleeper passing frequency, and dynamic train-track interaction (Esveld 2001, Punetha et al. 2021), and this approach has been widely adopted to capture the track dynamic behaviour (Li et al. 1998, Kennedy et al. 2013, Nimbalkar et al. 2016, Indraratna et al. 2018, Punetha et al. 2020), among others. To determine a dynamic wheel load, P_d for a moving train due to DAF, an empirical relationship as proposed by Li et al. (1998) based on American Railway Engineering Association (AREA) is used, as given:

$$P_d = \emptyset P \tag{15}$$

where, P_d = Dynamic wheel load; P = Static wheel load; $\emptyset$ = Dynamic amplification factor and is determined by:

$$\emptyset = 1 + 5.21\frac{v}{D} \tag{16}$$

However, in this equation, v = train speed (km/h); and D = wheel diameter in mm (970mm considered in this study).

Equation (14) is employed for the cases of four-carriage train loading (P =10-tonne) moving at four different speeds (v = 60, 100, 150, and 200 km/h) with five different track stiffness values (k = 5, 10, 20, 40 and 80 MN/m/m), and the calculated vertical displacements of rail tracks are presented in Fig. 7. Comparing Fig. 6 and Fig. 7, it can be noted that the maximum track settlement (w_{max}) for k =5MN/m/m under P =10 tonnes increases from 8mm to 10.1mm, 11.7mm, 13.8mm, and 15.8mm under the train speed of 60 km/h, 100km/h, 150km/h, and 200km/h, respectively. A similar increasing trend can also be observed for other stiffness values. Hence, a further increase in track settlement under each wheel load can be observed, demonstrating the enhanced dynamic loading effect of moving loads.

Fig. 8 shows the calculated maximum vertical displacements of the tracks subjected to train (P =10 tonnes), moving at various speeds and track stiffnesses in comparison with similar data reported from case studies. It can be seen that the effect of moving train loading (e.g. settlement) increases with the increase in train speed, however, this effect becomes less noticeable for higher track stiffness. The comparison with some past studies (Karlsson et al. 2016, Lamas-Lopez et al. 2017, Lei 2017, Coelho et al. 2018) shows that despite different sites and loading conditions, there are similar trends in the increase in vertical displacements with the increase in train speeds. It can also be observed from Fig. 8 that the absolute differential settlement (Δw) between any two tracks with different stiffness values, increases with the increase in train speed. For example, for a stiffness variation of Δk = 75MN/m/m (from 5 to 80 MN/m/m) is Δw=10.5mm and Δw=17.8mm for the train moving at v=100km/h and v=300km/h, respectively. This indicates that the trains moving at higher speeds can lead to higher differential settlements.

Research Approach and Methodology for Track at Transition Zones

Problem Identification

In order to identify the severity of the problem, a typical track transition between a soft track (conventional ballast track) and a stiff track (concrete bridge deck) as shown Fig. 9(a), is considered in this study. This is a common transition when a traditional ballast track changes to a concrete slab section, for instance when crossing a bridge. In this model, the soft track is considered as a layered structure that consists of rails, concrete sleepers, ballast, sub-ballast and subgrade, whereas the track on concrete bridge deck has no sub-ballast or soft subgrade layers, becomes considerably much stiffer than a ballasted track. An abrupt change in track stiffness has been assumed to be the main effect of this track transition where overall (global) track stiffness, k_s of the stiff track suddenly changes to k_b which is the total track stiffness of ballast track as shown in Fig. 9(b). Primarily, both the stiffness values are known or they can be determined from field measurements. A total variation in track stiffness values ($\Delta k = k_s - k_b$) at a given transition can then be determined accordingly. This stiffness variation (Δk) serves as an input parameter for the design of the track transition zone.

Effect of Stiffness Variation at Track Transition

To investigate the effect of sudden stiffness variation on the track settlement at track transition, a base case of track transition (one-step transition) is adopted where the stiffness suddenly changes from k = 80 to 5 MN/m/m at $x = 0$ (i.e. the Junction point). This case was solved analytically for four-carriage loading (P =10-tonne) using Equation (13) where:

$$k = k_s = 80 \text{ MN/m/m} \qquad \text{for } x \leq 0$$

and

$$k = k_b = 5 \text{ MN/m/m} \qquad \text{for } x > 0$$

In order to capture the most critical condition with respect to differential settlements, half of the train loading was considered on one side of the track junction and half on the other side as shown in Fig. 10. The settlements (w) under each wheel loading are calculated and plotted along the track length. It can be noted that the maximum settlements on the stiffer and softer side of the track transition are 0.69mm and 8.05mm, respectively. It shows that the settlements on ballasted track are far greater than those on the stiffer track (concrete bridge deck) resulting in a substantial differential settlement at this location. Based on the above values, the maximum differential settlement, Δw_{max} (normalised) is found up to 11.7 times the settlement on a stiffer track. This would lead to increased dynamic loading impact causing accelerated degradation of track geometry and material. Hence, to mitigate these problems, this differential settlement needs to be reduced to a certain allowable limit through the provision of an effective transition zone.

Wheel Load Effect on the Differential Settlement at Track Transition

In order to investigate the effect of wheel loading on the differential settlement for the typical transition case, Equation (13) is analysed for P=10, 12.5, 15 and 20-tonnes wheel loading. It is noted that the differential settlement increases significantly with the increase in wheel loading. The results obtained for track settlement on both sides of the track transition are plotted in Fig. 10(b), showing an enhanced differential settlement with increased wheel loading. This Figure also designates a linear trend for increased settlement with an increase in wheel loading. Hence, it can be concluded that the load amplification at any track transition results in higher differential settlement and this trend is expected to continue if proper mitigation measures are not implemented. A multi-step transition is now introduced as a mitigation measure to minimise the differential settlement and this is discussed in the following section.

Proposed Solution

To minimise the differential settlements at track transitions, a smooth variation of stiffness values between adjacent sections is required. This can be achieved by providing a properly designed transition zone comprising multiple segments ensuring gradual variation in their stiffness values. A novel analytical approach for the provision of a multi-step transition zone comprised of various transition segments with varying stiffness values is introduced in this study. The concept of this proposed novel approach for transition zone design is illustrated in Fig. 11. It presents a transition zone of length L, between a slab track with stiffness k_0 (k_{max}) and a ballasted track with stiffness k_{n+1} (k_{min}). This transition zone is comprised of a given number of transition segments (n), each with length (l). A step-by-step process of the proposed approach and the practical design guidelines for a transition zone is given in the following sections. In addition, a complete flow chart for the practical design steps based on the proposed approach is given in Fig. 12.

In this approach, values of n and l are firstly determined, followed by the determination of stiffness of each segment (k_i). The value of k_i is then obtained through an iterative process for a gradual change of Δk and is set to minimise the differential settlement (Δw_i) between any two consecutive transition segments as an optimisation criterion. In this study k_i is proposed based on the total stiffness variation at any track transition Δk, and the total number of segments and their lengths (the length of each segment has been assumed constant for simplicity) in the proposed transition zone, as given:

$$k_i = \Delta k \times e^{(0.0007L-0.1)\times X_i} + k_{n+1} \tag{17}$$

where, k_i = Track stiffness value of segment i (MN/m/m); $\Delta k = k_s - k_b$: Total stiffness variation at track transition (MN/m/m); $L = n \times l$: Total length of the transition zone (m); n: Total number of transition segments; l: Length of each segment (m); X_i: Distance of endpoint of segment i from track junction, $i = 1$ to n.

The output parameters from the proposed method of analysis are: (i) the number of transition steps, (ii) the length of each step, and (iii) the stiffness of each step. The first two parameters will decide the total length of the transition zone, while the third parameter helps to determine the type and specifications of materials used in that specific segment. The overall track stiffness is determined from a combined stiffness of various track elements (Powrie et al. 2016), as given in Equation (10) and the stiffness of track substructural components can be determined using Equation (11).

New Design Criterion to Optimise Differential Settlement

An allowable differential settlement ($\Delta w_{allowed}$) is adopted as the main design criterion for transition zones using the proposed approach. This criterion suggests that the settlement at the track with lesser stiffness (w_{soft}) at a given transition zone (e.g. between any two consecutive transition segments) must be less than the α (alpha) times the settlement at the stiffer track (w_{stiff}):

$$w_{soft} \leq \alpha \times w_{stiff} \quad \text{or} \quad w_i \leq \alpha \times w_{i-1} \tag{18}$$

$$\Delta w_{allowed} = \frac{w_{soft}}{w_{stiff}} = \frac{w_i}{w_{i-1}} \leq \alpha \tag{19}$$

where α is the allowable settlement enhancement factor indicating the maximum allowable differential settlement (normalised) between any two consecutive track segments in a transition zone. The selection of α depends upon design criteria for a given track condition and is recommended to be closer to 1 to avoid large differential settlements. In this study, the authors select values of α as 1.5 and 2 for the two worked-out examples provided at the end.

Hence, the number of transition segments (n) and the length of each segment (l) need to be selected to ensure that $\Delta w_{allowed}$ criterion (Equation (19) is fulfilled. However, if this criterion is not fulfilled for any two consecutive segments, the number of segments needs to be increased until this criterion is satisfied for all the segments. This criterion also serves as the initial check for the provision of a transition zone at any track transition. Hence, it can be suggested that there is no specific requirement to provide any transition zone if the settlement on the softer side of any track junction is not more than α times the settlement occurring on the stiffer side.

Step-by-Step Design Guidelines

Based on the solution for track transition, the following steps are introduced for the design of track transition under train loadings. A summary of the steps is presented in Fig. 12.

Step 1: Find the stiffness variation for the given track transition

$$\Delta k = k_0 - k_{n+1} \tag{20}$$

Step 2: Calculate the maximum settlement for each track segment using Equations (14) to (16) and then maximum differential settlement, Δw_{max} at the given track junction is determined as:

$$\Delta w_{max} = \frac{w_{n+1}}{w_0} \tag{21}$$

Step 3: Apply differential settlement check:

$$\Delta w_{max} \leq \Delta w_{allowed} = \alpha \tag{22}$$

However, if $\Delta w_{max} \leq \Delta w_{allowed}$ then the transition zone is not required. Otherwise, move to step 4.

Step 4: Assume the number of segments, n in the transition zone (i.e., starting with $n = 1$)

Step 5: Assume the length, l of each segment (l =$5m - 10m$, as suggested by Lei (2017))

Step 6: Calculate the stiffness value for each segment as given:

$$k_i = \Delta k \times e^{(0.0007L - 0.1) \times X_i} + k_{n+1} \tag{23}$$

where $i = 1$ to n, $\quad L = n \times l$, $\quad X_i =$ distance of endpoint of segment i from $x = 0$

Step 7: Calculate differential settlement for every two consecutive segments under various train speeds and load, Δw_i

$$\Delta w_i = \frac{w_i}{w_{i-1}} \tag{24}$$

where, w_i: Maximum settlement under wheel load at transition segment i

Step 8: Apply differential settlement check for $\Delta w_{i,\,max}$

$$\Delta w_{i,\ max} \leq \Delta w_{allowed} = \alpha \tag{25}$$

if $\Delta w_{i,\ max} > \Delta w_{allowed}$, go back to Step 4 with $n = n + 1$; otherwise, if $\Delta w_{i,\ max} \leq \Delta w_{allowed}$: Total transition length, $L = n \times l$, and stiffness of each segment = k_i

Results and Discussion

Differential Settlement for Multi-step Transition

In order to minimize the differential settlement resulting from a one-step track transition case, a novel approach is introduced for the provision of multi-step transition zones. In this study, a 40m long transition zone, as suggested by Hu et al. (2019), has been adopted for a smooth variation of track stiffness. Furthermore, a five-step transition zone comprising four transition segments ($n = 4$), with length of 10m each ($l = 10m$) is introduced and the stiffness value of each segment was calculated using Equation (17), which gives $k_1 = 41.5$ MN/m/m, $k_2 = 22.8$ MN/m/m, $k_3 = 13.6$ MN/m/m, and $k_4 = 9.2$ MN/m/m, respectively. The corresponding settlements are then determined using Equation (13), considering the appropriate length and stiffness value for each segment. A four-carriage static train with 10-tonne wheel loading is considered in this analysis and the predicted vertical displacements along the track are presented in Fig. 13(a), showing the maximum settlement under each wheel load (w_p) and its variation with respect to the stiffness of each segment. It is also noted that with the provision of a transition zone, the track settlement changes gradually from one section to the other. It is observed that without a proper transition zone, the maximum normalised differential settlement (Δw_i) was computed as 11.7 (Fig. 10a), however this Δw_i is significantly reduced to the maximum value of only 1.8, for any two consecutive segments, when a five-step transition zone is considered. Hence, knowing the settlement values under each wheel load, the differential settlement, Δw_i for all the transition segments can be determined by Equation (24).

Additionally, these differential settlement values (Δw_i) can be used as a criterion for optimising the design of transition zones.

Design Optimisation through Differential Settlement Criterion

In order to design the transition zone for the given stiffness variation, the differential settlement (Δw_i) is optimised using normalised settlement between various segments. The settlement under a given wheel load, (P_p) is normalised with the settlement under the previous wheel (P_{p-1}) of a four-carriage train moving from left to right (stiff to soft). Fig. 13(b) shows this normalised settlement for each wheel load along the track. A zero differential settlement line has been added to Fig. 13(b) where the normalised settlement is equal to 1. This line indicates that the settlement under any specific wheel load is the same as the settlement under the previous wheel load, which is mainly due to the same stiffness sections thus resulting in zero differential settlement, such as for $P_1, P_7,\ P_{11}, P_{14}$, among others. Another line has also been added to demarcate the maximum allowed settlement at a level where the normalised settlement is equal to 2 (α has been assumed as 2 in this example). This line represents the transition zone design criterion, ensuring that the settlement under any specific wheel load must not increase twice the settlement under the previous wheel load. It is observed that differential settlement occurs only when two consecutive wheels are on different track segments with varying stiffness, such as for $P_4, P_6, P_8, P_{10},$ & P_{12}. However, the values are below the allowable differential settlement ($\Delta w_{allowed}$) that indicates the proper provision of the five-step transition zone through smooth stiffness variation.

Design of Transition Zone through Numerical modelling

An abrupt change in structural characteristics at the track transition makes the design of the transition zone complicated to be fully handled using an analytical approach. Additionally, the BOEF theory has several limitations for the dynamic response analysis of track substructure, especially regarding the nonlinearity of the substructure layers. Although, the simple BOEF or mass-spring-dashpot model can be utilised to understand the simple behaviour of track transition through the analytical model.

Whereas, extensive calculations are required to study the dynamic response at track transitions analytically considering various characteristics, of all the supporting layers individually, including non-linearity, inhomogeneity, and plasticity, among others (Indraratna et al. 2019). However, numerical modelling can investigate the mechanical behaviour of such complex tracks under dynamic loading conditions (Zhang et al. 2016, Heydari-Noghabi et al. 2017).

Hence, in order to develop a numerical model for the design of the transition zone, the 2D FEM layered model was further updated to incorporate the one-step transition from a stiff structure to a soft as shown in Fig. 14(a). This figure simulates the track transition shown in Fig. 9(a), with an abrupt change in stiffness values from 80MN/m/m to 5MN/m/m. The transition divides the model into two portions; the left represents the stiff structure with 80MN/m/m and the right with 5MN/m/m. The rail has been modelled as a continuous beam for the whole 120m length of the model and has been kept the same for both the tracks along with the sleepers. The mechanical properties of all the materials are kept the same as given in Table 1, except the E values of ballast, sub-ballast and subgrade that were adjusted to match the track equivalent stiffness on both sides of the transition (Table 2).

The deformation contour of this transition model under the effect of multiple wheels (P =10t) loading is given in Fig. 14(b). Results obtained from the FEM show that the softer track undergoes higher deformation (8.4 mm) compared to stiffer track (0.2 mm). The vertical displacements under the effect of multiple loading and sudden stiffness variation, obtained through both analytical and numerical modelling approaches, are presented in Fig. 14(c). This shows a good agreement between analytical and numerical results, showing that the FEM model can be used in determining a differential settlement for a given stiffness variation at transition zones.

The authors understand that a comprehensive 3D Numerical model for optimizing railway transition zones would be ideal albeit much greater computational time and effort. While the current 2D model is a stepping stone towards this goal by serving as a preliminary assessment tool, it is still adequate for determining the needs of the transition zone. Where the longitudinal direction has a very long dimension compared to the transverse direction, the true 3D condition indeed becomes close to 2D

Plane Strain that still serves the purpose, as explained by many past studies (Powrie et al. 2007, Sadeghi et al. 2010).

Only vertical strains are calculated in this 2D model (plane strain assuming a very long track length) with an out-of-plane thickness of one meter, to determine the differential settlement which is crucial for design optimization. Given the simplified 2D plane strain model adopted in the current analysis, a reasonable agreement has still been achieved between the 2D FEM prediction and the authors' analytical method. The authors are still on the progress of developing a more comprehensive 3D track model, but its discussion is beyond the scope of this paper. The current 2D model can reduce numerical complexity and provides a faster and more efficient means to establish the preliminary design, which can subsequently be further optimized for various site conditions using a 3D model.

The 2D FEM model is further developed for the transition zone design optimisation, incorporating a multi-step transition zone obtained through the analytical approach introduced in this study. In this regard, the total number of transition segments, their length and stiffness values are determined by following the first six steps of the proposed approach (Fig. 12). These values are then incorporated into the FEM model to update it for a multistep transition zone, which can be analysed in detailed considering various characteristics of the supporting layers under dynamic loads of moving trains in different directions. In this study, the numerical model (Fig. 14a) was further updated for a 40m long five-step transition zone with four transition segments as shown in Fig. 15(a). The model represents a gradual variation of abrupt stiffness change from k_0 to k_{n+1} through the provision of a transition zone consisting of four segments with stiffness values varying from k_1 to k_4. It is worth mentioning that the stiffness values of these segments are determined through the analytical approach introduced in this study, and they are then utilised to calculate the material properties of substructural layers as given in Table 2.

This model was solved for the vertical displacements under the effect of multiple wheel loading (P =10t) and the results of deformation contour are shown in Fig. 15(b). It can be observed that there is a gradual increase in the intensity of settlements and the spread of deformation contours from stiff track to soft track substructure. The comparison for the vertical displacements of tracks subjected to

16 wheels loading obtained through analytical and numerical modelling approaches is presented in Fig. 15(c). It is seen that the predicted settlements obtained from FEM simulation are in good agreement with those calculated by the analytical method, indicating the reliability of the numerical model that can be applied in transition zone design optimisation, considering the multiple wheel loading and layered track substructure.

Practical Implications

A transition zone is essential to minimize the effect of abrupt variations in track stiffness, for instance, in the case of a gradual transition from a ballast section to a much stiffer slab track or a bridge deck. In essence, minimising the differential settlement through a gradual variation of stiffness over a number of transition zone sections is key for ensuring track stability. As explained in the flow chart (Fig. 12), the key input parameters must correctly assess and quantify the optimum track stiffness on both sides of the transition based on fundamental mechanics, and where possible supported by field data. Indeed, the proposed method will also assist in implementing the appropriate ground improvement methods to attain the required magnitudes of stiffness, as explained further via two worked-out examples below.

Worked-out Design Example-1: Design of Transition Zone between Slab Track and Ballast Track

To demonstrate the capability of the given approach, the design of a transition zone between a slab track and a ballast track is carried out. The track stiffness values for slab track and ballast track have been considered as k_{slab} =350 MN/m/m, and $k_{ballast}$ =70 MN/m/m as considered by Ngamkhanong et al. (2020).

Input design parameters:

- Stiffness of stiffer track section (slab track), $k_{slab} = k_0 = 350$ MN/m/m
- Stiffness of soft track section (ballast track), $k_{ballast} = k_{n+1} = 70$ MN/m/m
- 30-tonne train axle loading, $P_{Axle} = 30$ tonne
- Train speed, $v = 70$ km/h
- Allowable settlement enhancement factor, $\alpha = 1.5$

Design calculation:

Step 1: Find a stiffness variation for the given track transition using Equation (20):

$$\Delta k = k_0 - k_{n+1} = 280 \text{ MN/m/m}$$

Step 2: In order to check the requirement of a transition zone, we will find the differential settlement ratio at the given track junction using Equations (14)-(16), which result in:

$$\Delta w_{max} = \frac{w_{n+1}}{w_0} = \frac{1.95}{0.6} = 3.25$$

Step 3: Apply differential settlement check:

$$\Delta w_{max} = 3.25 > \Delta w_{allowed} = \alpha = 1.5$$

Check failed, so we need to design the track transition following the next steps

Step 4: $n = 1$

Step 5: $l = 5m$

Step 6: Calculate stiffness value for segment 1 using Equation (23):

$$k_1 = 280 \times e^{(0.0007\times5-0.1)\times5} + 70 = 242.8 \text{ MN/m/m}$$

Step 7: Calculate the differential settlement ratio for every consecutive segment

$$\Delta w_1 = \frac{w_1}{w_0} = 1.3$$

$$\Delta w_2 = \frac{w_2}{w_1} = 2.5$$

Step 8: Apply differential settlement check:

$$\Delta w_{max} = \Delta w_2 = 2.5 > \Delta w_{allowed} = \alpha = 1.5$$

Check failed, so we need to go back to Step 4 with increased n as $n = n + 1$

Step 4a: $n = 1 + 1 = 2$

Step 5a: $l = 5m$

Step 6a: $k_1 = 245.9$ MN/m/m, $k_2 = 180.5$ MN/m/m

Step 7a: $\Delta w_1 = 1.29$, $\Delta w_2 = 1.25$ and $\Delta w_3 = 1.99$

Step 8a: $\Delta w_{max} = \Delta w_3 = 1.99 > \Delta w_{allowed} = \alpha = 1.5$

Check failed, so we need to go back to Step 4 with increased n as $n = n + 1$

Step 4b: $n = 2 + 1 = 3$

Similarly, following steps 5b to 7b, we get

Step 8b: $\Delta w_{max} = \Delta w_4 = 1.69 > \Delta w_{allowed} = \alpha = 1.5$

Check failed, so we need to go back to step 4 with increased n as $n = n + 1$

Step 4c: $n = 3 + 1 = 4$

Step 5c: $l = 5m$

Step 6c: $k_1 = 252.1$ MN/m/m, $k_2 = 188.5$ MN/m/m, $k_3 = 147.1$ MN/m/m, & $k_4 = 120.1$ MN/m/m

Step 7c: $\Delta w_1 = 1.27$, $\Delta w_2 = 1.23$, $\Delta w_3 = 1.1$, $\Delta w_4 = 1.16$, & $\Delta w_5 = 1.48$

Step 8c: Applying differential settlement check:

$$\Delta w_{max} = \Delta w_5 = 1.48 \leq \Delta w_{allowed} = \alpha = 1.5$$

Check passed

This shows the maximum differential settlement between any two consecutive segments in the newly designed transition zone is less than the allowable limit. Hence, the final design of the transition zone considering a gradual stiffness variation at the junction of the given slab and ballast track is as follows:

- Total number of transition segments, $n = 4$ (which gives the total number of transition steps as 5)
- Length of each transition segment, $l = 5$m
- The total length of the transition zone, $L = n \times l = 20$m

Track stiffness of each segment:

$k_0 = 350\ \mathrm{MN/m/m}$, $k_1 = 252.1\ \mathrm{MN/m/m}$, $k_2 = 188.5\ \mathrm{MN/m/m}$, $k_3 = 147.1\ \mathrm{MN/m/m}$, $k_4 = 120.1\ \mathrm{MN/m/m}$, and $k_5 = 70\ \mathrm{MN/m/m}$

Worked-out Design Example-2: Stiffness Variation and Transition Steps

In order to investigate the effect of total stiffness variation and the number of transition steps in any transition zone, the differential settlement for a multi-step transition zone is calculated (adopting Equation 21) for twelve different cases. Three types of transition zones are considered based on their number of transition steps: (i) 4-step transition, (ii) 5-step transition, and (iii) 6-step transition. Each of them is then solved for four different cases based on the total stiffness variation between stiff (concrete bridge deck) and soft (ballast) track sections; (i) $\Delta k = 75$ MN/m/m considering $k_s = 80$ MN/m/m, & $k_b = 5$ MN/m/m, (ii) $\Delta k = 60$ MN/m/m considering $k_s = 80$ MN/m/m, & $k_b = 20$ MN/m/m, (iii) $\Delta k = 45$ MN/m/m considering $k_s = 80$ MN/m/m, & $k_b = 35$ MN/m/m, and (iv) $\Delta k = 30$ MN/m/m considering $k_s = 80$ MN/m/m, & $k_b = 50$ MN/m/m.

The results of all these twelve cases for normalised differential settlement between various transition segments (steps) are presented in Fig. 16. It is seen that there is a significant decrease in differential settlement for the fourth step of a 4-step transition with $\Delta k = 75$ MN/m/m, by increasing the number of transition steps from 4 to 5. Based on Fig. 16, for all these cases, there is a substantial decrease in differential settlement with the increase in the number of steps in a transition zone. Similarly, it can also be noted that irrespective of the total number of steps, the higher the stiffness variation at track transition, the larger the differential settlement occurring between various transition segments. This worked-out example demonstrates that the differential settlement within the transition zone can be controlled up to the maximum allowed value (e.g. $\alpha = 2$, for this example) by increasing the length of the transition zone with the addition of more transition segments for a gradual variation of track stiffness along the critical track sections.

Limitations

The analytical approach and the corresponding methodology for tracks at transition zones presented in the current study have certain limitations, including: (i) In the analytical approach, the substructure soil conditions (layered track) were assumed using a representative spring having an equivalent stiffness, k; (ii) the allowable settlement enhancement factor, α (i.e. limiting strain value) has to be determined before the calculation process, and; (iii) Principal stress rotation as well as increased track vibrations as a result of the moving wheel effect has not been considered in this study.

Conclusions

In this study, minimising differential settlement caused by sudden stiffness variation was analysed based on a beam on an elastic foundation subjected to various train loading conditions using analytical and numerical modelling approaches. Due to the abrupt changes in track stiffness, a significant differential settlement occurred at the transitions, which was further exacerbated by load amplification. The outcomes of this study including the salient flow chart representation can inspire better design solutions, as well as revised specifications and practical guidelines for track transition zones. In summary, finding the appropriate length of transition zones to gradually transform the track stiffness should reduce the differential settlement at these critical locations to minimise track degradation.

The following specific conclusions can be drawn based on the model outputs:

- The analytical and numerical modelling outcomes showed that an increase in track stiffness from k=5MN/m/m (ballasted track) to k=80MN/m/m (slab track) would result in a significant reduction in track settlements, w_{max} (i.e., reduced from w_{max}=4.9 mm to w_{max}=0.6 mm, respectively). A maximum differential settlement (Δw_{max}) nearly 12 times that of the settlement on the stiffer side could be evaluated. From a stability perspective, such differential values would be detrimental in relation to long heavy-haul trains, hence the imperative need for designing interim transition zones.
- The track settlements increased with an increase in train speed. For instance, under a given wheel load of P=10 tonnes and track stiffness k=5 MN/m/m, the analytical model showed an increase in maximum track settlement from w_{max}=8 mm to w_{max}=15.8 mm, when the train speed increased from 60 km/h to 200km/h. This demonstrated the enhanced dynamic loading effect attributed to moving loads.
- The absolute differential settlement (Δw) between any two tracks having different values of stiffness increased with the train speed. For a given stiffness variation of Δk = 75MN/m/m, the values of Δw were calculated as 10.5mm and 17.8mm for speeds of v=100km/h and

v=300km/h, respectively. Such analyses confirmed that trains moving at higher speeds will lead to higher differential settlement.

- An optimization process was introduced to determine the required stiffness (k_i) for each segment to compute the minimum differential settlement. This process ensured that the number of transition steps could be selected optimally so that the differential settlement between any two consecutive segments would be less than the allowable settlement enhancement factor, α.
- The FEM results of vertical displacements were found to be in good agreement with the analytical results. As the actual moving wheel loading was simulated on a layered track (with measured geotechnical parameters), the soil-structure interaction and geotechnical aspects of a typical track could be properly captured in this FEM small-strain analysis. This validation proves that the BOEF approach can be reliably used for analysing the behaviour at transition zones for a given set of computational factors (number of steps, length, stiffness), thus a minimal differential settlement could be achieved.

The current study provides a significant extension for design rejuvenation of transition zones by minimising the differential settlement at any two consecutive transition segments. The outcomes of this study can assist the practitioners to design transition zone taking to account the total length with the number of transition steps and appropriate stiffness values and their variation along the track.

Data Availability Statements

Some or all data, models, or code that support the findings of this study are available from the corresponding author upon reasonable request (Data for plotting Figures, parts of programming code, etc.).

Acknowledgements

This research was carried out by the Australian Research Council Industrial Transformation Training Centre for Advanced Technologies in Rail Track Infrastructure (IC170100006) and DP220102862, funded by the Australian Government. The authors thank the Australian Rail Track Corporation (ARTC) for their continuous support and cooperation. The authors also appreciate the insightful collaboration and assistance of the Australasian Centre for Rail Innovation (ACRI) and Snowy Mountains Engineering Corporation (SMEC), in particular the comments and thoughtful advice provided for the current study.

References

Abadi, T., L. L. Pen, A. Zervos, and W. Powrie. 2019. "Effect of sleeper interventions on railway track performance." Journal of Geotechnical and Geoenvironmental Engineering 145(4): 04019009. https://doi.org/10.1061/(ASCE)1090-0241(2008)134:10(1558).

Aggestam, E., and J. C. Nielsen. 2019. "Multi-objective optimisation of transition zones between slab track and ballasted track using a genetic algorithm." Journal of Sound and Vibration 446: 91-112. https://doi.org/10.1016/j.jsv.2019.01.027.

Berggren, E. G., A. M. Kaynia, and B. Dehlbom. 2010. "Identification of substructure properties of railway tracks by dynamic stiffness measurements and simulations." Journal of Sound and Vibration 329(19): 3999-4016. https://doi.org/10.1016/j.jsv.2010.04.015.

Choi, J. 2013. "Influence of track support stiffness of ballasted track on dynamic wheel-rail forces." Journal of transportation engineering 139(7): 709-718. https://doi.org/10.1061/(ASCE)TE.1943-5436.0000543.

Choudhury, D., R. K. Bharti, S. Chauhan, and B. Indraratna. 2008. "Response of multilayer foundation system beneath railway track under cyclic loading." Journal of Geotechnical and Geoenvironmental Engineering 134(10): 1558-1563. https://doi.org/10.1061/(ASCE)1090-0241(2008)134:10(1558).

Chumyen, P., D. Connolly, P. Woodward, and V. Markine. 2022. "The effect of soil improvement and auxiliary rails at railway track transition zones." Soil Dynamics and Earthquake Engineering 155: 107200. https://doi.org/10.1016/j.soildyn.2022.107200.

Coelho, B., J. Priest, and P. Hölscher. 2018. "Dynamic behaviour of transition zones in soft soils during regular train traffic." Journal of Rail and Rapid Transit 232(3): 645-662. https://doi.org/10.1177/0954409716683078.

Dahlberg, T. 2010. "Railway track stiffness variations - consequences and countermeasures." International Journal of Civil Engineering 8(1): 1-12. http://ijce.iust.ac.ir/article-1-420-en.html.

Dimitrovová, Z., and J. Varandas. 2009. "Critical velocity of a load moving on a beam with a sudden change of foundation stiffness: Applications to high-speed trains." Computers & Structures 87(19-20): 1224-1232. https://doi.org/10.1016/j.compstruc.2008.12.005.

Esmaeili, M., H. Heydari-Noghabi, and M. Kamali 2018. "Numerical investigation of railway transition zones stiffened with auxiliary rails." Institution of Civil Engineers-Transport, Thomas Telford Ltd.

Esveld, C. 2001. Modern railway track. 2nd edition. MRT-Productions, The Netherlands.

Frohling, R., H. Scheffel, and W. Ebersöhn. 1996. "The vertical dynamic response of a rail vehicle caused by track stiffness variations along the track." Vehicle System Dynamics: International Journal of Vehicle Mechanics and Mobility 25(S1): 175-187. https://doi.org/10.1080/00423119608969194.

Gallego Giner, I., and A. López Pita. 2009. "Numerical simulation of embankment—structure transition design." Proceedings of the Institution of Mechanical Engineers, Part F: Journal of Rail and Rapid Transit 223(4): 331-343. https://doi.org/10.1243/09544097JRRT234.

Galvín, P., A. Romero, and J. Dominguez. 2010. "Vibrations induced by hst passage on ballast and non-ballast tracks." Soil Dynamics and Earthquake Engineering 30(9): 862-873. https://doi.org/10.1016/j.soildyn.2010.02.004.

Hendry, M. T. 2007. "Train-induced dynamic response of railway track and embankments on soft peaty foundations."

Heydari-Noghabi, H., J. N. Varandas, M. Esmaeili, and J. Zakeri. 2017. "Investigating the influence of auxiliary rails on dynamic behavior of railway transition zone by a 3d train-track interaction model." Latin American Journal of Solids and Structures 14: 2000-2018. https://doi.org/10.1590/1679-78253906.

Heydari-Noghabi, H., J. Zakeri, M. Esmaeili, and J. Varandas. 2018. "Field study using additional rails and an approach slab as a transition zone from slab track to the ballasted track." Journal of Rail and Rapid Transit 232(4): 970-978. https://doi.org/10.1177/0954409717708527.

Hibbitt, D., B. Karlsson, and P. Sorensen. 2014. "Abaqus standard user’s and reference manuals." Dassault Systèmes.

Hu, P., C. Zhang, S. Wen, and Y. Wang. 2019. "Dynamic responses of high-speed railway transition zone with various subgrade fillings." Computers and Geotechnics 108: 17-26. https://doi.org/10.1016/j.compgeo.2018.12.011.

Huang, H., and B. Brennecke. 2013. "Track stiffness transition zone studied with three-dimensional sandwich track model." Transportation Research Record: Journal of the Transportation Research Board(2374): 136-142. https://doi.org/10.3141/2374-16.

Indraratna, B., and T. Ngo 2018. Ballast railroad design: Smart-uow approach. CRC Press, United States. https://doi.org/10.1201/9780429504242

Indraratna, B., M. B. Sajjad, T. Ngo, A. G. Correia, and R. Kelly. 2019. "Improved performance of ballasted tracks at transition zones: A review of experimental and modelling approaches." Transportation Geotechnics 21: 100260. https://doi.org/10.1016/j.trgeo.2019.100260

Indraratna, B., W. Salim, and C. Rujikiatkamjorn 2011. Advanced rail geotechnology–ballasted track. CRC press, Netherlands. https://doi.org/10.1201/b10861.

Karlsson, N., and M. Hjelm 2016. "Dynamic response of railway bridges subjected to high speed trains-parametrical case studies." MS Thesis, CHALMERS University of Technology, Sweden.

Kennedy, J., P. Woodward, G. Medero, and M. Banimahd. 2013. "Reducing railway track settlement using three-dimensional polyurethane polymer reinforcement of the ballast." Construction and Building Materials 44: 615-625.

Kenney, J. 1954. "Steady-state vibrations of beam on elastic foundation for moving load." J. appl. Mech. 21: 359-364.

Kerr, A. D., and B. E. Moroney. 1993. "Track transition problems and remedies." Bulletin American Railway Engineering Association(742): 267-298.

Kouroussis, G., D. P. Connolly, and O. Verlinden. 2014. "Railway-induced ground vibrations–a review of vehicle effects." International Journal of Rail Transportation 2(2): 69-110. https://doi.org/10.1080/23248378.2014.897791.

Lamas-Lopez, F., Y.-J. Cui, N. Calon, S. C. D'Aguiar, and T. Zhang. 2017. "Impact of train speed on the mechanical behaviours of track-bed materials." Journal of Rock Mechanics and Geotechnical Engineering 9(5): 818-829. https://doi.org/10.1016/j.jrmge.2017.03.018.

Lamprea-Pineda, A. C., D. P. Connolly, and M. F. Hussein. 2021. "Beams on elastic foundations–a review of railway applications and solutions." Transportation Geotechnics: 100696. https://doi.org/10.1016/j.trgeo.2021.100696.

Le Pen, L., G. Watson, W. Powrie, G. Yeo, P. Weston, and C. Roberts. 2014. "The behaviour of railway level crossings: Insights through field monitoring." Transportation Geotechnics 1(4): 201-213. https://doi.org/10.1016/j.trgeo.2014.05.002.

Lei, X. 2017. High speed railway track dynamics. Springer, Singapore. https://doi.org/10.1007/978-981-10-2039-1

Lei, X., and B. Zhang. 2010. "Influence of track stiffness distribution on vehicle and track interactions in track transition." Journal of Rail and Rapid Transit 224(6): 592-604. https://doi.org/10.1243/09544097JRRT318.

Li, D., and D. Davis. 2005. "Transition of railroad bridge approaches." Journal of Geotechnical and Geoenvironmental Engineering 131(11): 1392-1398. https://doi.org/10.1061/(ASCE)1090-0241(2005)131:11(1392).

Li, D., and E. T. Selig. 1998. "Method for railroad track foundation design. I: Development." Journal of geotechnical and geoenvironmental engineering 124(4): 316-322. https://doi.org/10.1061/(ASCE)1090-0241(1998)124:4(316).

Li, D., and E. T. Selig. 1998. "Method for railroad track foundation design. Ii: Applications." Journal of geotechnical and geoenvironmental engineering 124(4): 323-329. https://doi.org/10.1061/(ASCE)1090-0241(1998)124:4(323).

López-Pita, A., P. F. Teixeira, C. Casas, L. Ubalde, and F. Robusté. 2007. "Evolution of track geometric quality in high-speed lines: Ten years experience of the madrid-seville line." Journal of Rail and Rapid Transit 221(2): 147-155. https://doi.org/10.1243/0954409JRRT62.

Lundqvist, A., and T. Dahlberg. 2005. "Load impact on railway track due to unsupported sleepers." Journal of Rail and Rapid Transit 219(2): 67-77. https://doi.org/10.1243/095440905X8790.

Luo, Q., M. Wei, Q. Lu, and T. Wang. 2021. "Simplified analytical solution for stress concentration ratio of piled embankments incorporating pile–soil interaction." Railway Engineering Science 29(2): 199-210. https://doi.org/10.1007/s40534-021-00236-z.

Mishra, D., H. Boler, E. Tutumluer, W. Hou, and J. P. Hyslip. 2017. "Deformation and dynamic load amplification trends at railroad bridge approaches: Effects caused by high-speed passenger trains." Transportation research record 2607(1): 43-53.

Mishra, D., Y. Qian, H. Huang, and E. Tutumluer. 2014. "An integrated approach to dynamic analysis of railroad track transitions behavior." Transportation Geotechnics 1(4): 188-200. https://doi.org/10.1016/j.trgeo.2014.07.001.

Mishra, D., E. Tutumluer, H. Boler, J. Hyslip, and T. Sussmann. 2014. "Railroad track transitions with multidepth deflectometers and strain gauges." Transportation Research Record: Journal of the Transportation Research Board(2448): 105-114. https://doi.org/10.3141/2448-13.

Namura, A., and T. Suzuki 2007. "Evaluation of countermeasures against differential settlement at track transitions." Quarterly Report of RTRI. 48**:** 176-182. https://doi.org/10.2219/rtriqr.48.176.

Ngamkhanong, C., Q. Y. Ming, T. Li, and S. Kaewunruen. 2020. "Dynamic train-track interactions over railway track stiffness transition zones using baseplate fastening systems." Engineering Failure Analysis 118: 104866. https://doi.org/10.1016/j.engfailanal.2020.104866.

Nicks, J. E. 2009. "The bump at the end of the railway bridge." PhD thesis, Texas A&M University.

Nimbalkar, S., and B. Indraratna. 2016. "Improved performance of ballasted rail track using geosynthetics and rubber shockmat." http://dx.doi.org/10.1061/(ASCE)GT.1943-5606.0001491.

Nimbalkar, S., B. Indraratna, S. K. Dash, and D. Christie. 2012. "Improved performance of railway ballast under impact loads using shock mats." Journal of geotechnical and geoenvironmental engineering 138(3): 281-294. https://doi.org/10.1061/(ASCE)GT.1943-5606.0000598.

OneSteel, L. 2017. "Rail track material: Steel rails and trak-lok steel sleeper systems, 2017."

Paixão, A., J. N. Varandas, E. Fortunato, and R. Calçada. 2018. "Numerical simulations to improve the use of under sleeper pads at transition zones to railway bridges." Engineering Structures 164: 169-182. https://doi.org/10.1016/j.engstruct.2018.03.005.

Pita, A. L., P. F. Teixeira, and F. Robuste. 2004. "High speed and track deterioration: The role of vertical stiffness of the track." Journal of Rail and Rapid Transit 218(1): 31-40. https://doi.org/10.1243/095440904322804411.

Plotkin, D., and D. Davis 2008. "Bridge approaches and track stiffness." U.S. Department of Transportation. https://rosap.ntl.bts.gov/view/dot/40230.

Powrie, W., and L. Le Pen 2016. A guide to track stiffness. University of Southampton.

Powrie, W., L. Yang, and C. R. Clayton. 2007. "Stress changes in the ground below ballasted railway track during train passage." Proceedings of the Institution of Mechanical Engineers, Part F: Journal of Rail and Rapid Transit 221(2): 247-262.

Priest, J., and W. Powrie. 2009. "Determination of dynamic track modulus from measurement of track velocity during train passage." Journal of geotechnical and geoenvironmental engineering 135(11): 1732-1740.

Punetha, P., S. Nimbalkar, and H. Khabbaz. 2020. "Analytical evaluation of ballasted track substructure response under repeated train loads." International Journal of Geomechanics 20(7): 04020093.

Punetha, P., S. Nimbalkar, and H. Khabbaz. 2021. "Simplified geotechnical rheological model for simulating viscoelasto ‐ plastic response of ballasted railway substructure." International Journal for Numerical and Analytical Methods in Geomechanics 45(14): 2019-2047. https://doi.org/10.1002/nag.3254.

Ramos, A., A. G. Correia, B. Indraratna, T. Ngo, R. Calçada, and P. A. Costa. 2020. "Mechanistic-empirical permanent deformation models: Laboratory testing, modelling and ranking." Transportation Geotechnics 23: 100326. https://doi.org/10.1016/j.trgeo.2020.100326.

Read, D., and D. Li 2006. "Design of track transitions." TCRP Research Results Digest.

Real, T., C. Zamorano, C. Hernández, J. García, and J. Real. 2016. "Static and dynamic behavior of transitions between different railway track typologies." KSCE Journal of Civil Engineering 20(4): 1356-1364. https://doi.org/10.1007/s12205-015-0635-2.

Sadeghi, J., and H. Askarinejad. 2010. "Development of nonlinear railway track model applying modified plane strain technique." Journal of transportation engineering 136(12): 1068-1074.

Sañudo, R., L. Dell'Olio, J. Casado, I. Carrascal, and S. Diego. 2016. "Track transitions in railways: A review." Construction and Building Materials 112: 140-157. https://doi.org/10.1016/j.conbuildmat.2016.02.084.

Sañudo, R., M. Miranda, and V. Markine. 2016. "The influence of train running direction and track supports position on the behaviour of transition zones." Transportation research procedia 18: 281-288. https://doi.org/10.1016/j.trpro.2016.12.037.

Selig, E. T., and D. Li. 1994. "Track modulus: Its meaning and factors influencing it." Transportation Research Record(1470).

Shahraki, M., C. Warnakulasooriya, and K. J. Witt. 2015. "Numerical study of transition zone between ballasted and ballastless railway track." Transportation Geotechnics 3: 58-67. https://doi.org/10.1016/j.trgeo.2015.05.001.

Shan, Y., S. Zhou, B. Wang, and C. L. Ho. 2020. "Differential settlement prediction of ballasted tracks in bridge–embankment transition zones." Journal of Geotechnical and Geoenvironmental Engineering 146(9): 04020075. https://doi.org/10.1061/(ASCE)GT.1943-5606.0002307.

Sung, D., S. Chang, and S. Kim. 2020. "Effect of additional anti-vibration sleeper track considering sleeper spacing and track support stiffness on reducing low-frequency vibrations." Construction and Building Materials 263: 120140. https://doi.org/10.1016/j.conbuildmat.2020.120140.

Tutumluer, E., Y. Qian, Y. M. Hashash, J. Ghaboussi, and D. D. Davis. 2013. "Discrete element modelling of ballasted track deformation behaviour." International Journal of Rail Transportation 1(1-2): 57-73. https://doi.org/10.1080/23248378.2013.788361.

Van Dalen, K. 2006. "Ground vibration induced by a high-speed train running over inhomogeneous subsoil, transition radiation in two-dimensional inhomogeneous elastic systems." Master`s thesis, Department of Structural Engineering, TUDelft.

Walker, R. T., and B. Indraratna. 2018. "Moving loads on a viscoelastic foundation with special reference to railway transition zones." International Journal of Geomechanics 18(11): 04018145.

Wang, H., M. Silvast, V. Markine, and B. Wiljanen. 2017. "Analysis of the dynamic wheel loads in railway transition zones considering the moisture condition of the ballast and subballast." Applied Sciences 7(12): 1208. https://doi.org/10.3390/app7121208.

Woodward, P. K., A. El Kacimi, O. Laghrouche, G. Medero, and M. Banimahd. 2012. "Application of polyurethane geocomposites to help maintain track geometry for high-speed ballasted railway tracks." Journal of Zhejiang University SCIENCE A 13(11): 836-849. https://doi.org/10.1631/jzus.a12isgt3

Zarembski, A., and J. Palese. 2003. "Transitions eliminate impact at crossings." Railway track and structures 99(8). http://worldcat.org/oclc/1763403.

Zhai, W., and H. True. 2000. "Vehicle-track dynamics on a ramp and on the bridge: Simulation and measurements." Vehicle System Dynamics 33: 604-615. https://doi.org/10.1080/00423114.1999.12063115.

Zhai, W., S. Wang, N. Zhang, M. Gao, H. Xia, C. Cai, and C. Zhao. 2013. "High-speed train–track–bridge dynamic interactions–part ii: Experimental validation and engineering application." International Journal of Rail Transportation 1(1-2): 25-41. https://doi.org/10.1080/23248378.2013.791497.

Zhai, W., H. Xia, C. Cai, M. Gao, X. Li, X. Guo, N. Zhang, and K. Wang. 2013. "High-speed train–track–bridge dynamic interactions–part i: Theoretical model and numerical simulation." International Journal of Rail Transportation 1(1-2): 3-24. https://doi.org/10.1080/23248378.2013.791498.

Zhang, T.-W., F. Lamas-Lopez, Y.-J. Cui, N. Calon, and S. C. D'Aguiar. 2017. "Development of a simple 2d model for railway track-bed mechanical behaviour based on field data." Soil Dynamics and Earthquake Engineering 99: 203-212. https://doi.org/10.1016/j.soildyn.2017.05.005.

Zhang, X., C. Zhao, and W. Zhai. 2016. "Dynamic behavior analysis of high-speed railway ballast under moving vehicle loads using discrete element method." International Journal of Geomechanics 17(7): 04016157.

Zhang, Y.-J., M. Murray, and L. Ferreira 1998. "A mechanistic approach for estimation of track modulus." Conference on Railway Engineering Proceedings: Engineering Innovation for a Competitive Edge: Engineering Innovation for a Competitive Edge, Central Queensland University Rockhampton, Qld.

Zhou, S., B. Wang, and Y. Shan. 2020. "Review of research on high-speed railway subgrade settlement in soft soil area." Railway Engineering Science 28(2): 129-145. https://doi.org/10.1007/s40534-020-00214-x.

Zuada Coelho, B. 2011. "Dynamics of railway transition zones in soft soils." Doctrol PhD Thesis, Delft University of Technology.

List of Figures

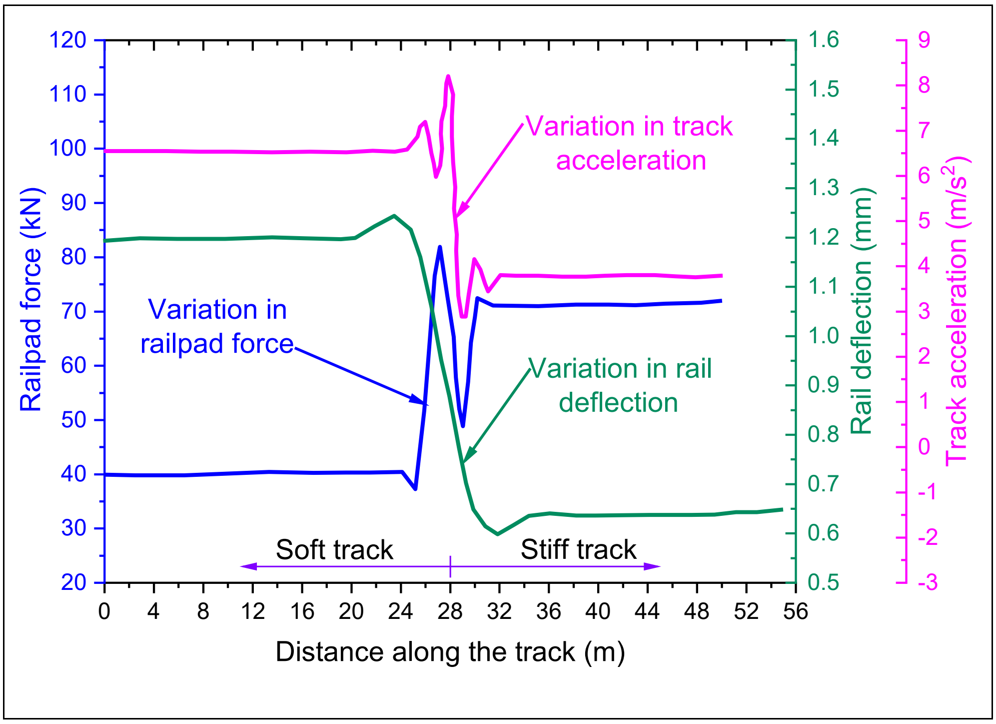

Fig. 1: Variation in track acceleration, rail deflection and rail pad force at track transition under moving loads

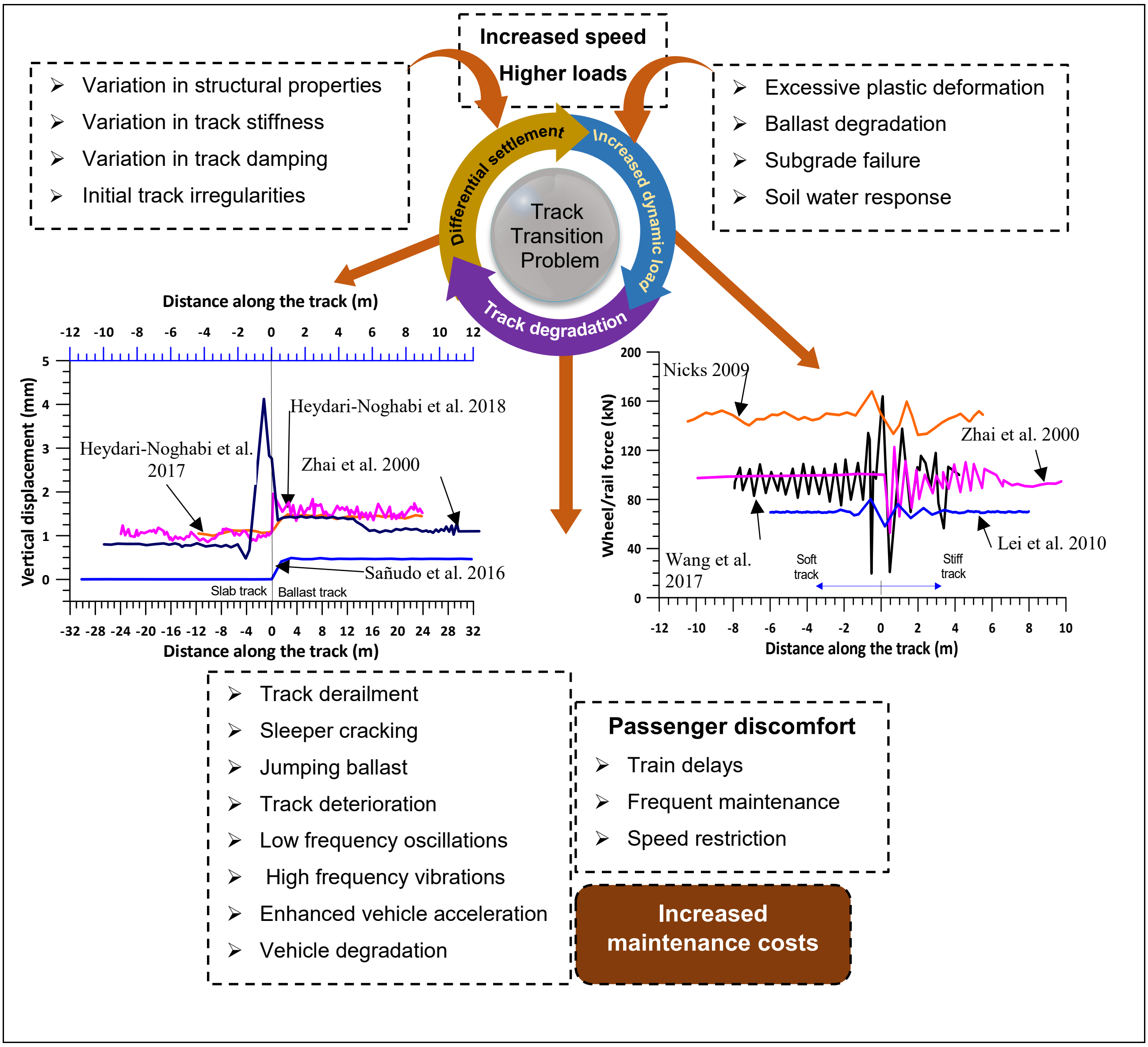

Fig. 2: Summarised track dynamics problems at track transitions: causes and effects

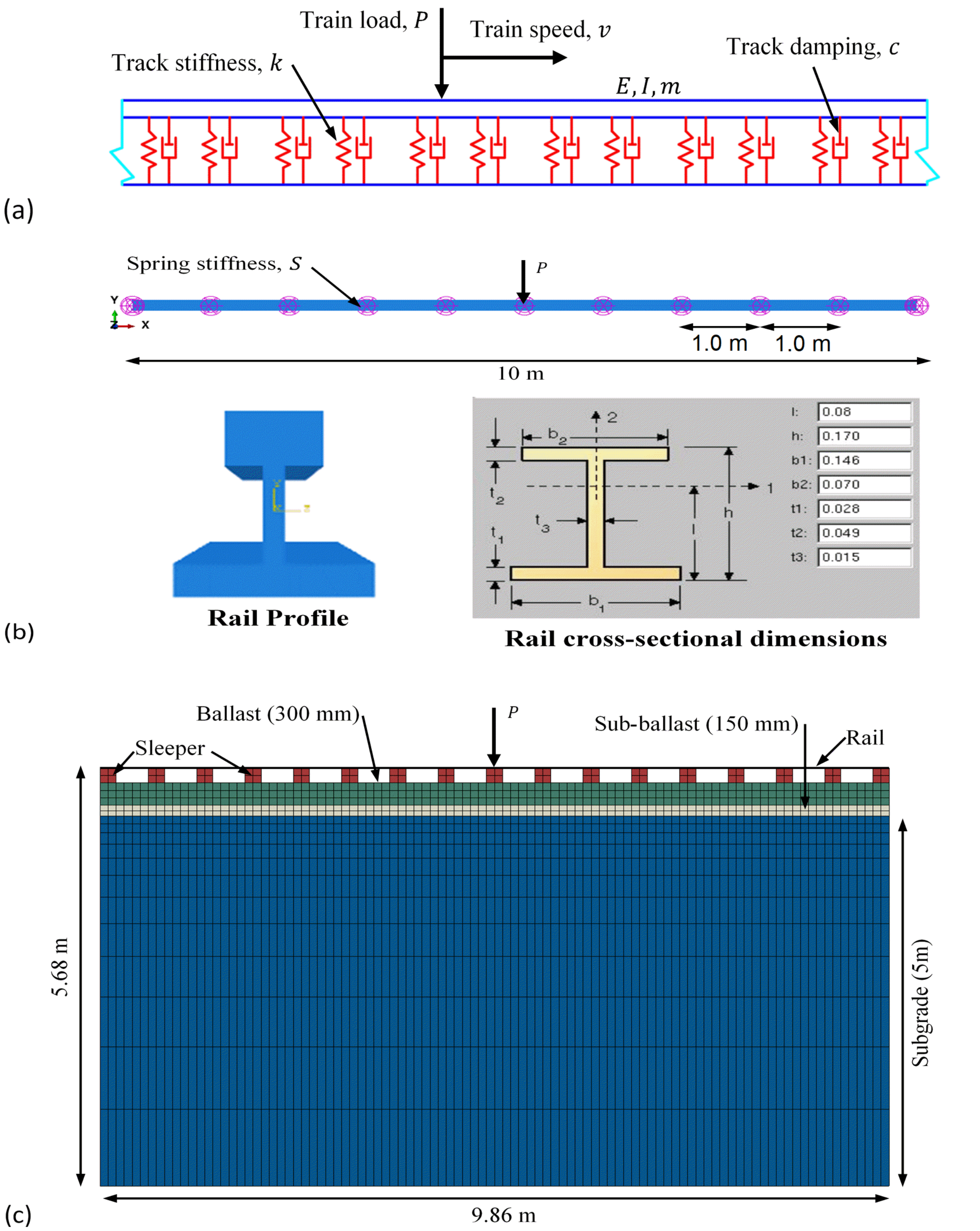

Fig. 3**:** (a) BOEF model (mass-spring-dashpot) for analytical modelling (b) Numerical model considering beam on springs, with rail profile and dimensions, after OneSteel (2017) (c) 2D FEM mesh model for conventional layered ballast track

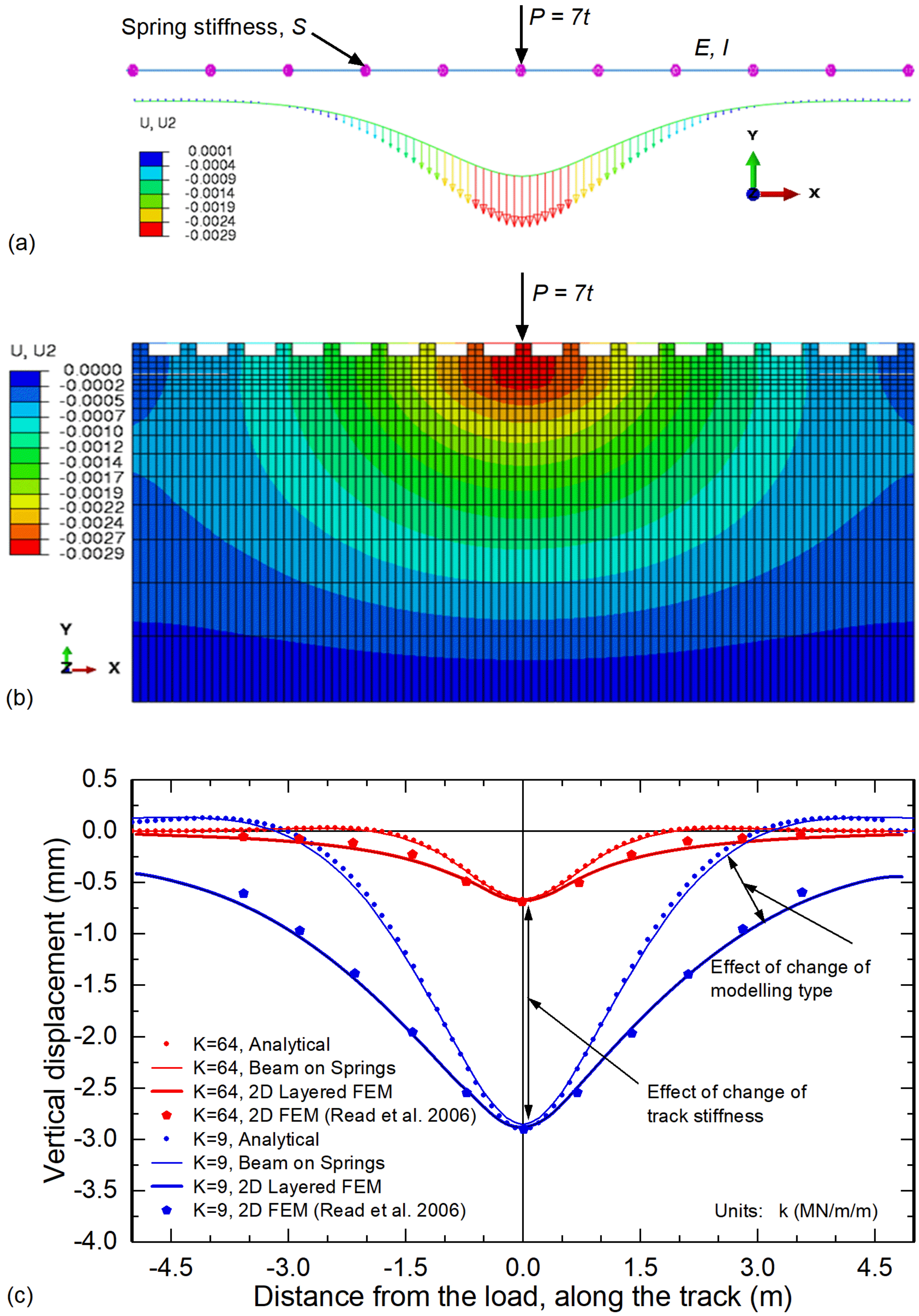

Fig. 4: (a) Deformation contours for 10m long steel beam resting on equally spaced springs with spring stiffness of 9MN/m, (b) Deformation contours for 2D FEM layered model with track stiffness as 9MN/m/m, (c) Comparison of vertical displacements of rail tracks for analytical and Numerical (i.e. beam on spring and 2D FEM layered) models.

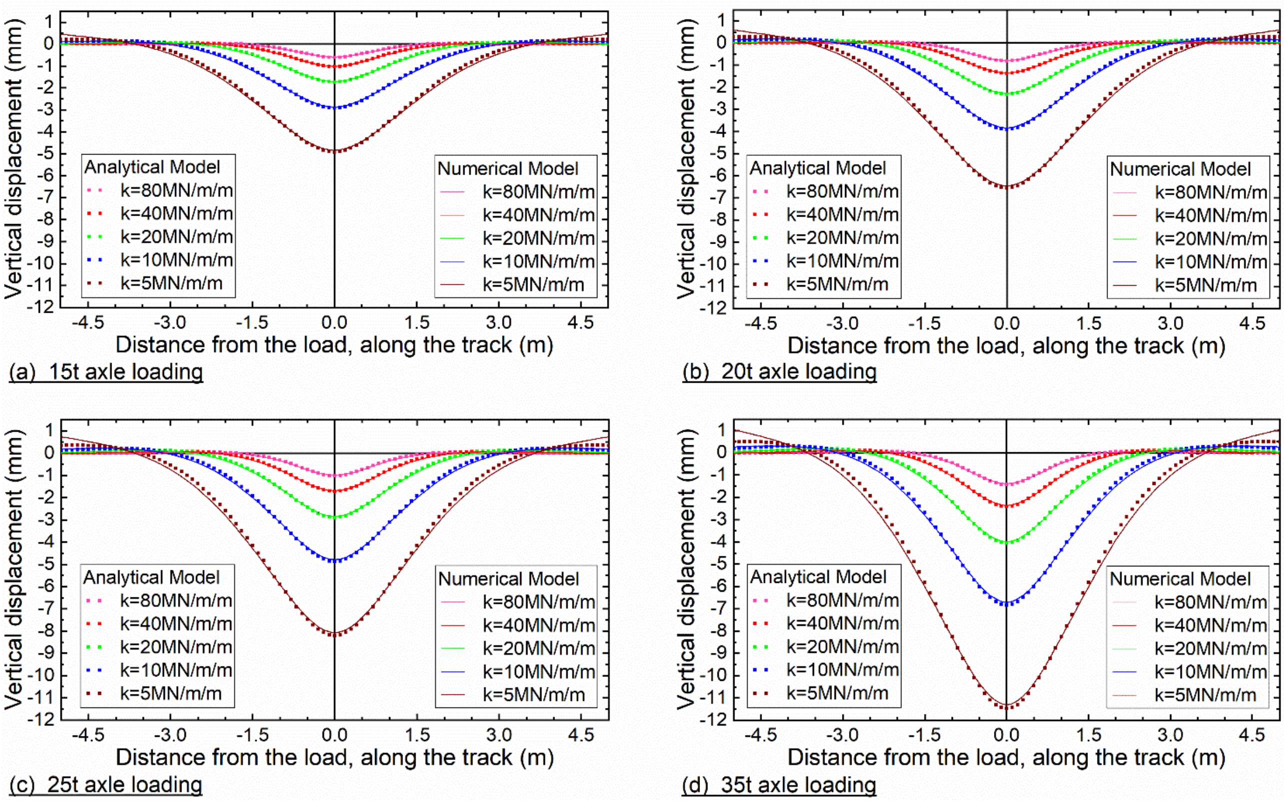

Fig. 5: Predicted vertical displacements of rail tracks subjected to different axle loadings; (a) 15-tonne axle load, (b) 20-tonne axle load, (c) 25-tonne axle load, and (d) 35-tonne axle load

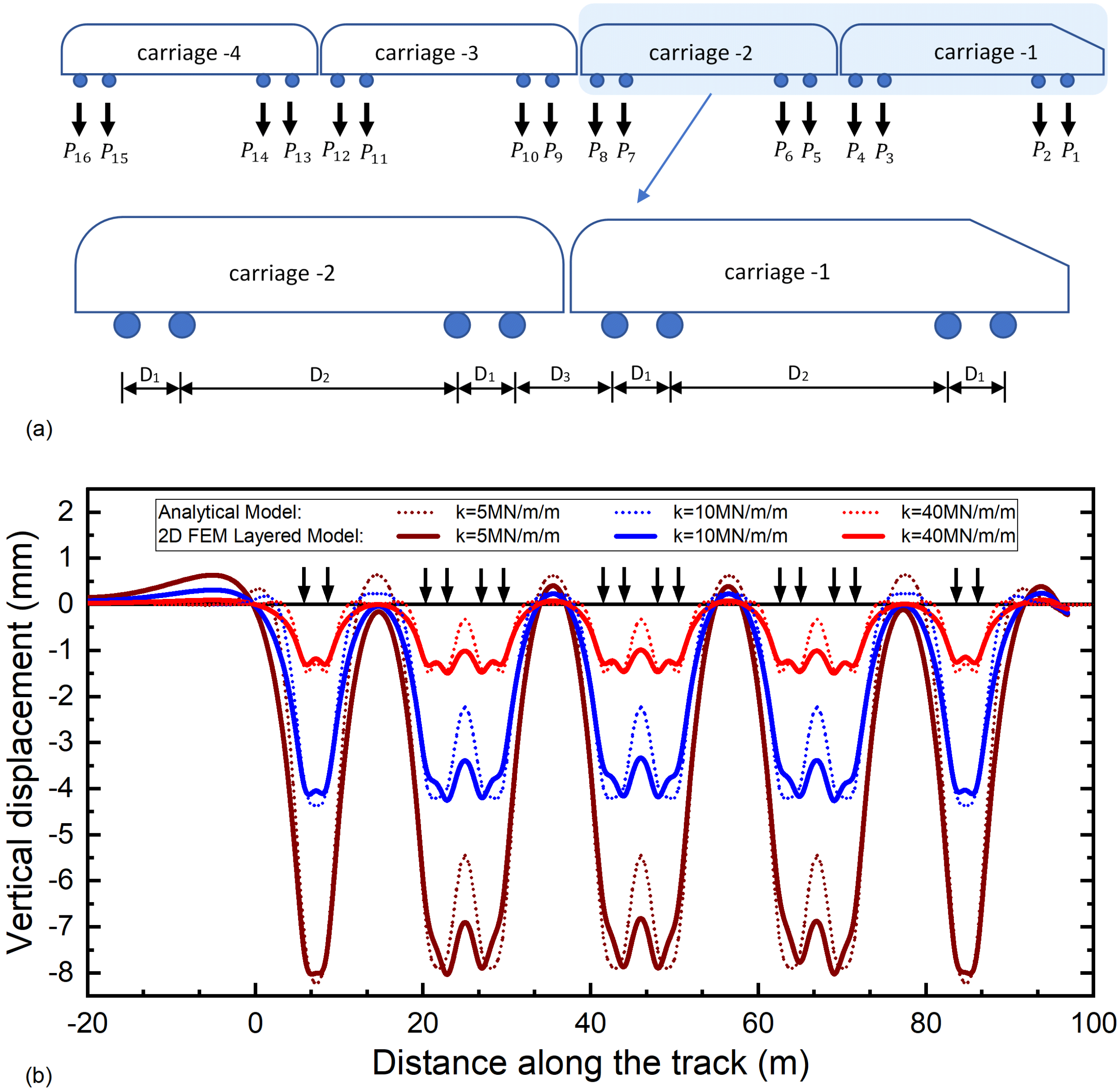

Fig. 6: (a) Four-carriage loading (b) Vertical displacements of rail tracks under four-carriage loading considering the effect of multiple loadings

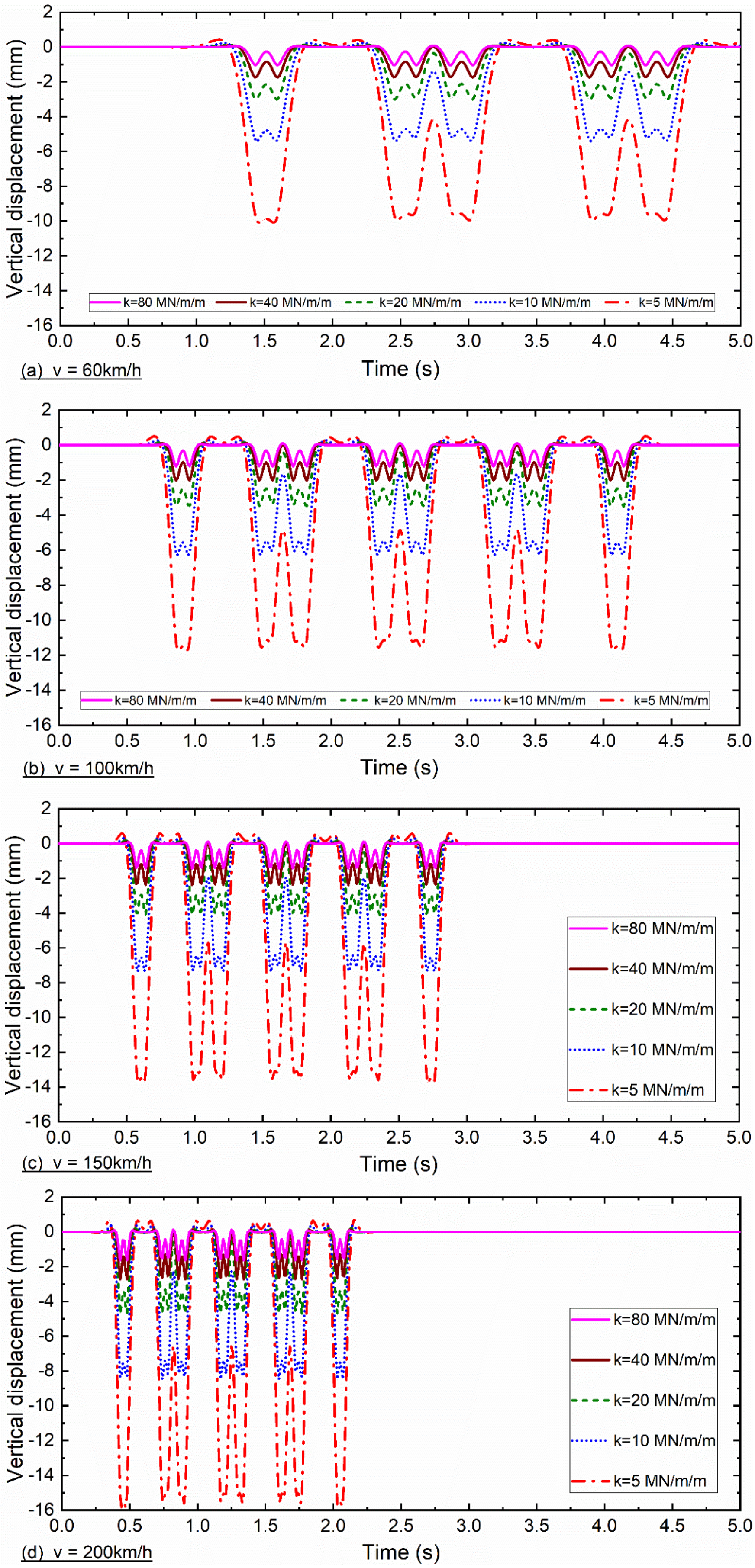

Fig. 7: Vertical displacements of the track calculated at various times considering 4- carriage (P = 10 tonnes) moving at various speeds; (a) v=60 km/h, (b) v=100 km/h, (c) v=150 km/h, and (d) v=200 km/h

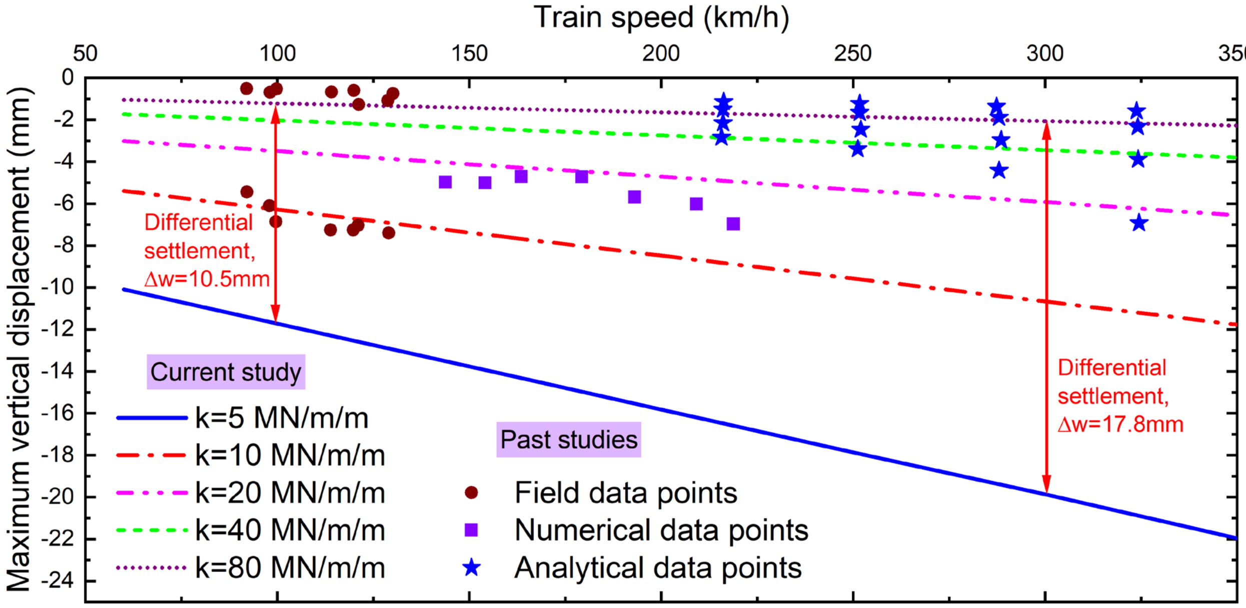

Fig. 8: Maximum vertical displacement of the rail track subjected to train moving at various speeds

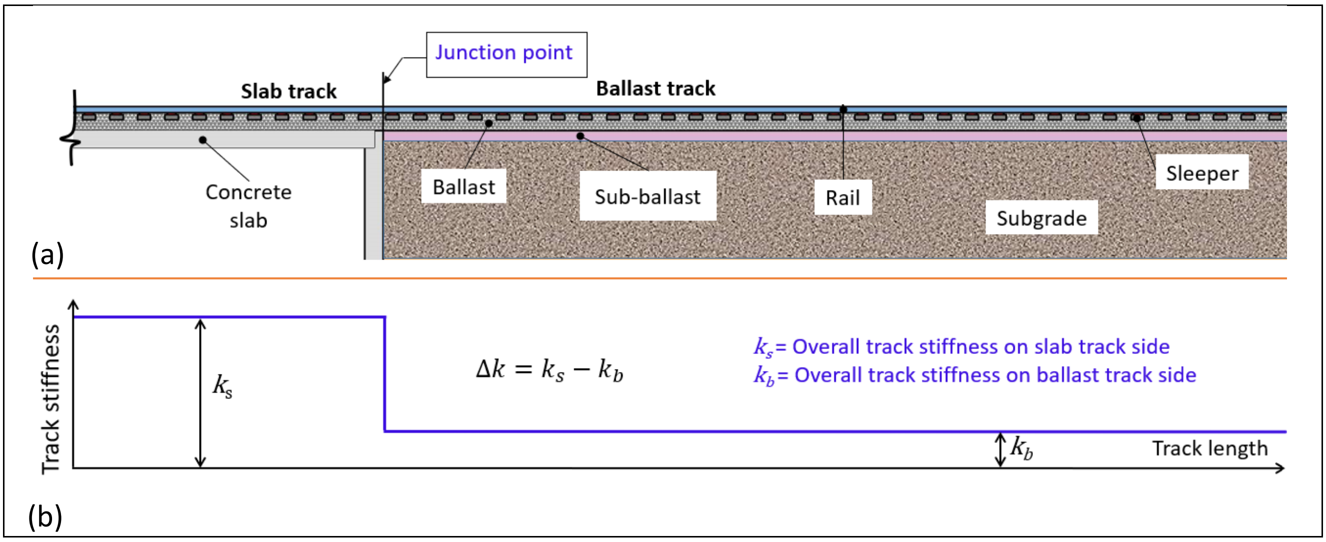

Fig. 9: (a) A typical track transition between slab track and ballast track, (b) Abrupt stiffness variation at track transition

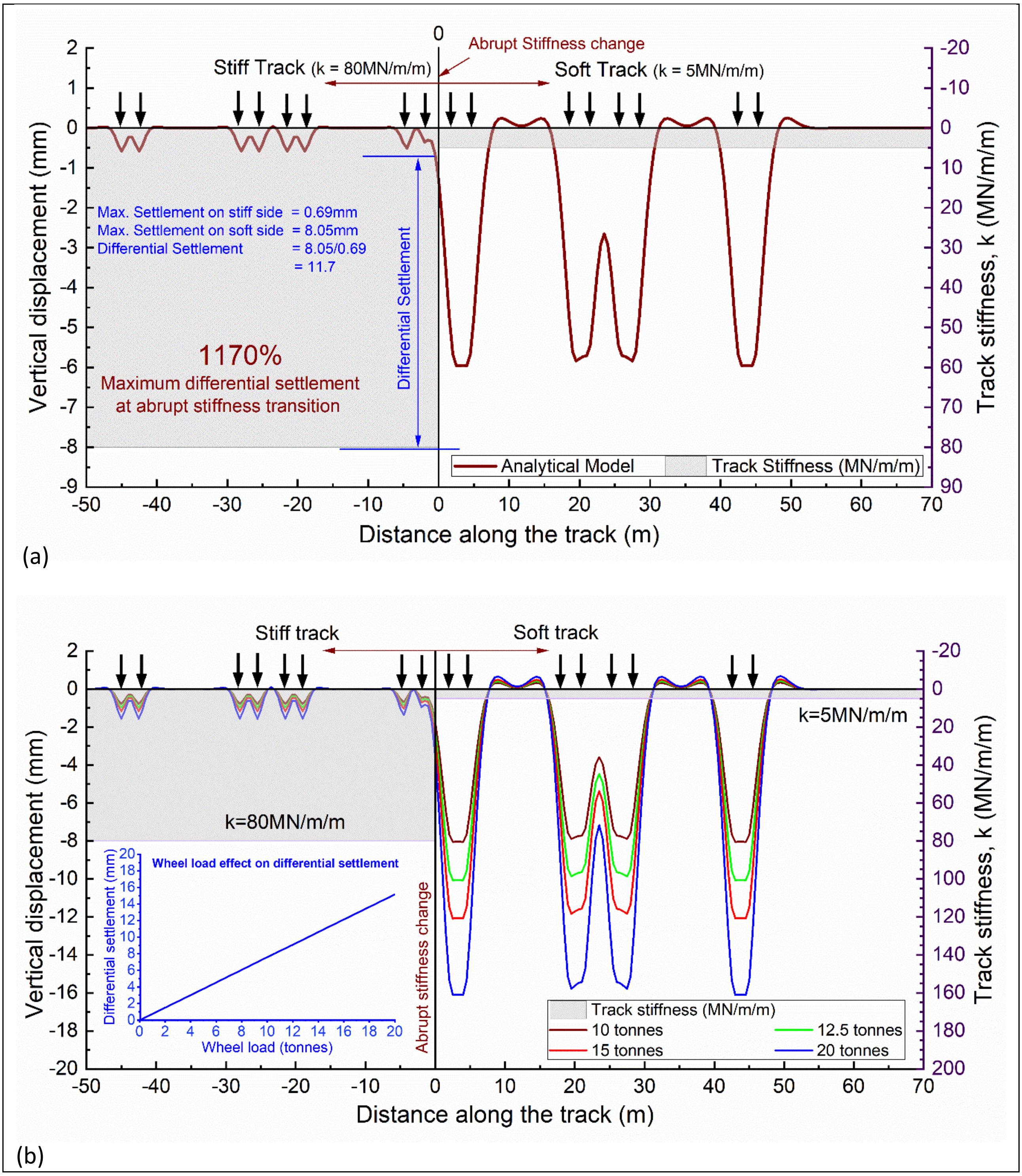

Fig. 10: (a) Calculated vertical displacement of rail track for one-step transition, stiffness varying from k=80 MN/m/m to k=5 MN/m/m under P=10 tonne; (b) The effect of wheel load (P) on differential settlements for one-step stiffness transition varying from k=80 MN/m/m (stiff track) to k=5 MN/m/m (ballasted track)

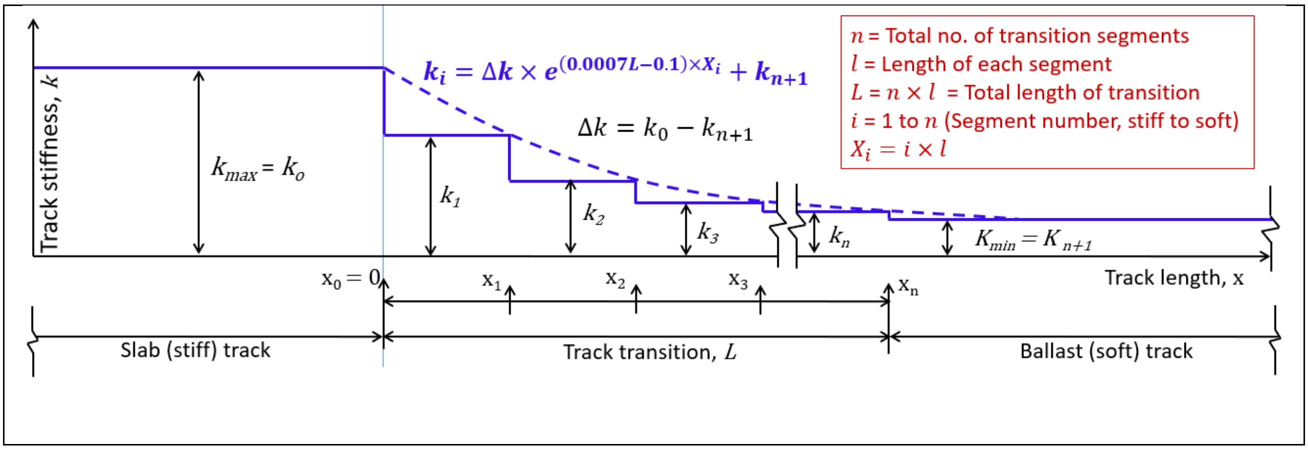

Fig. 11: Proposed transition zone design for smooth stiffness variation

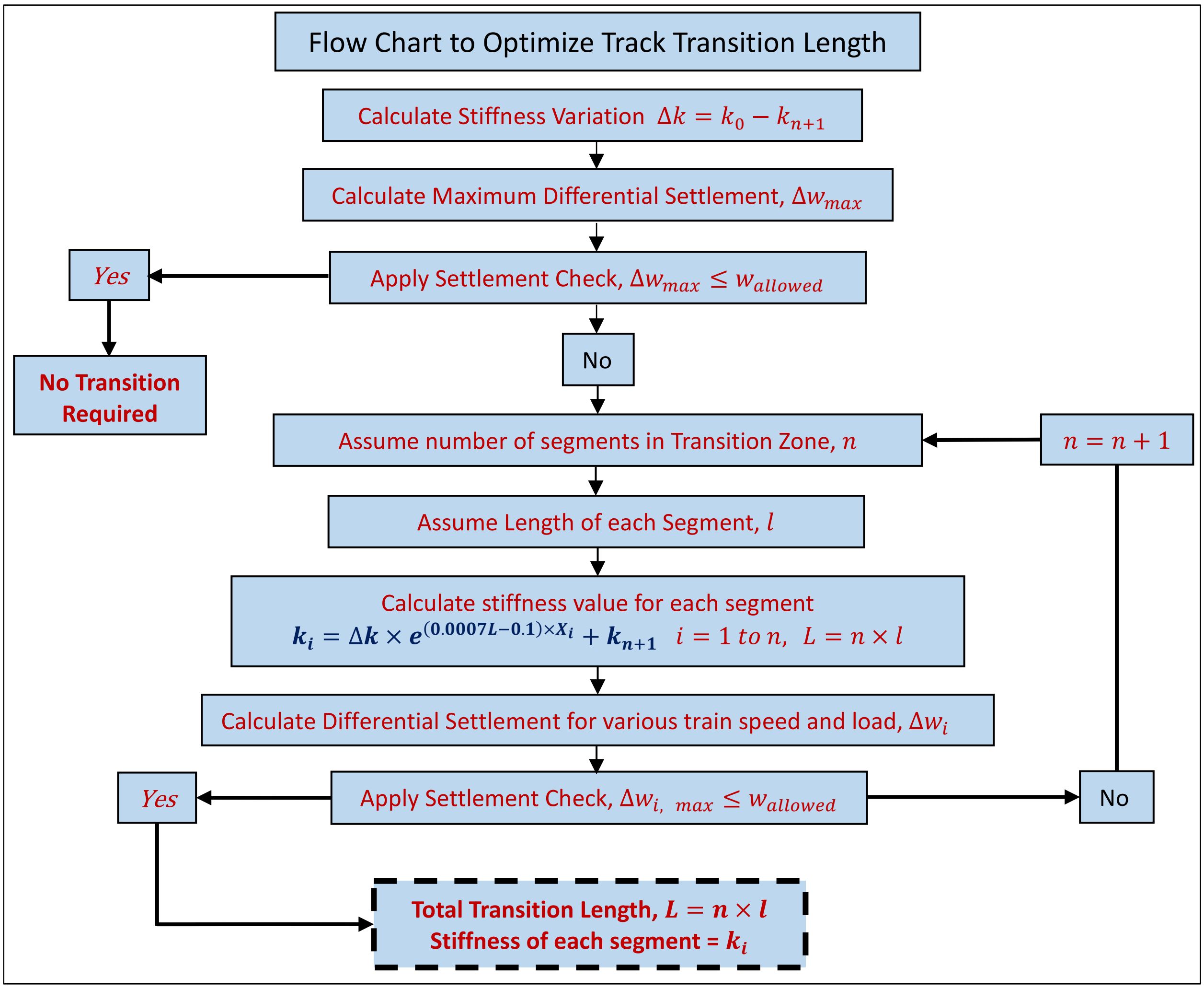

Fig. 12: Flow chart for the proposed novel approach for the design of track transition zone

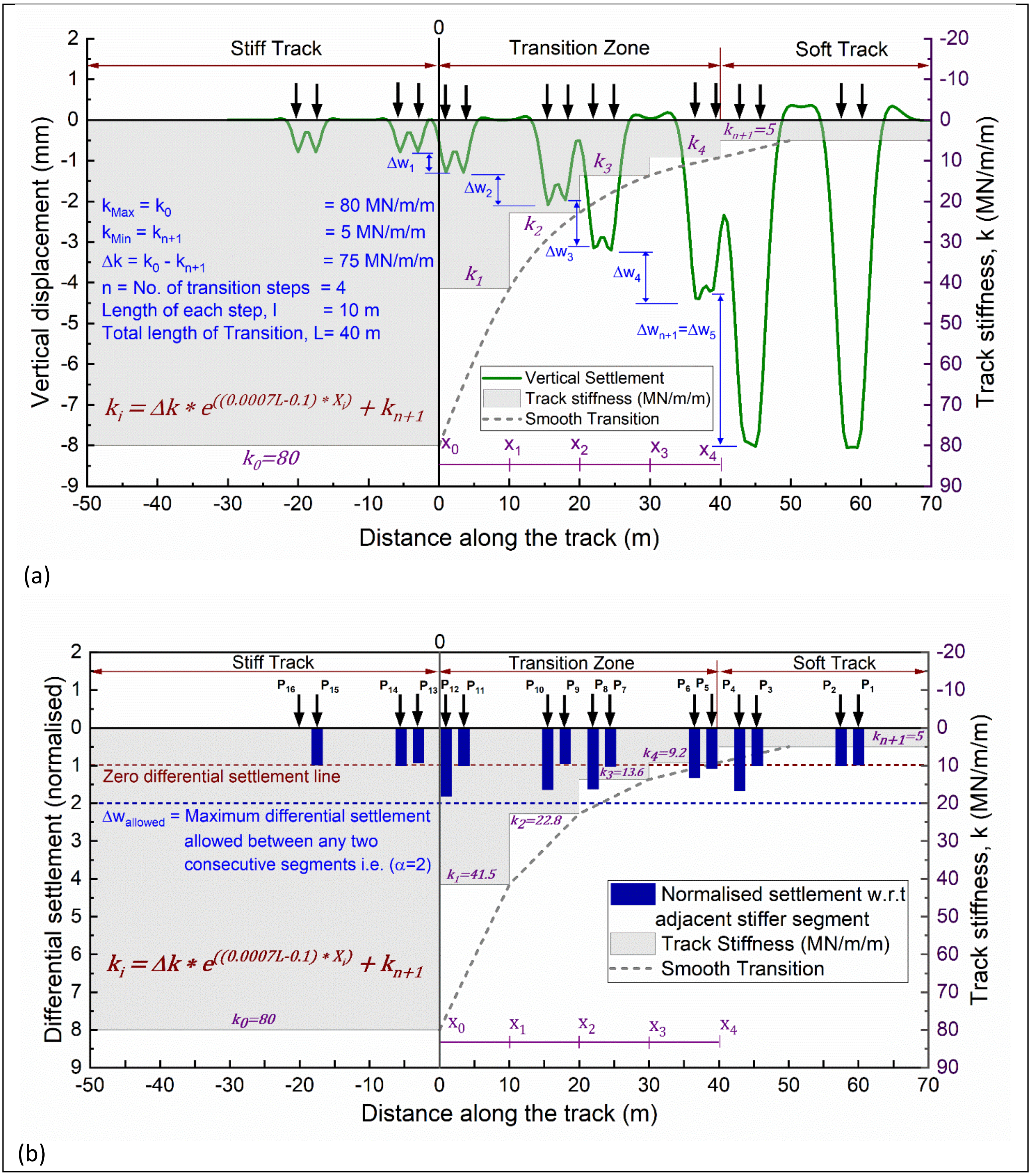

Fig. 13: (a) Rail deflection for a five-step transition zone under four-carriage static train loading with 10-tonne wheel loadings; (b) Normalised settlement for a five-step transition zone under four-carriage static train loading with 10-tonne wheel loadings

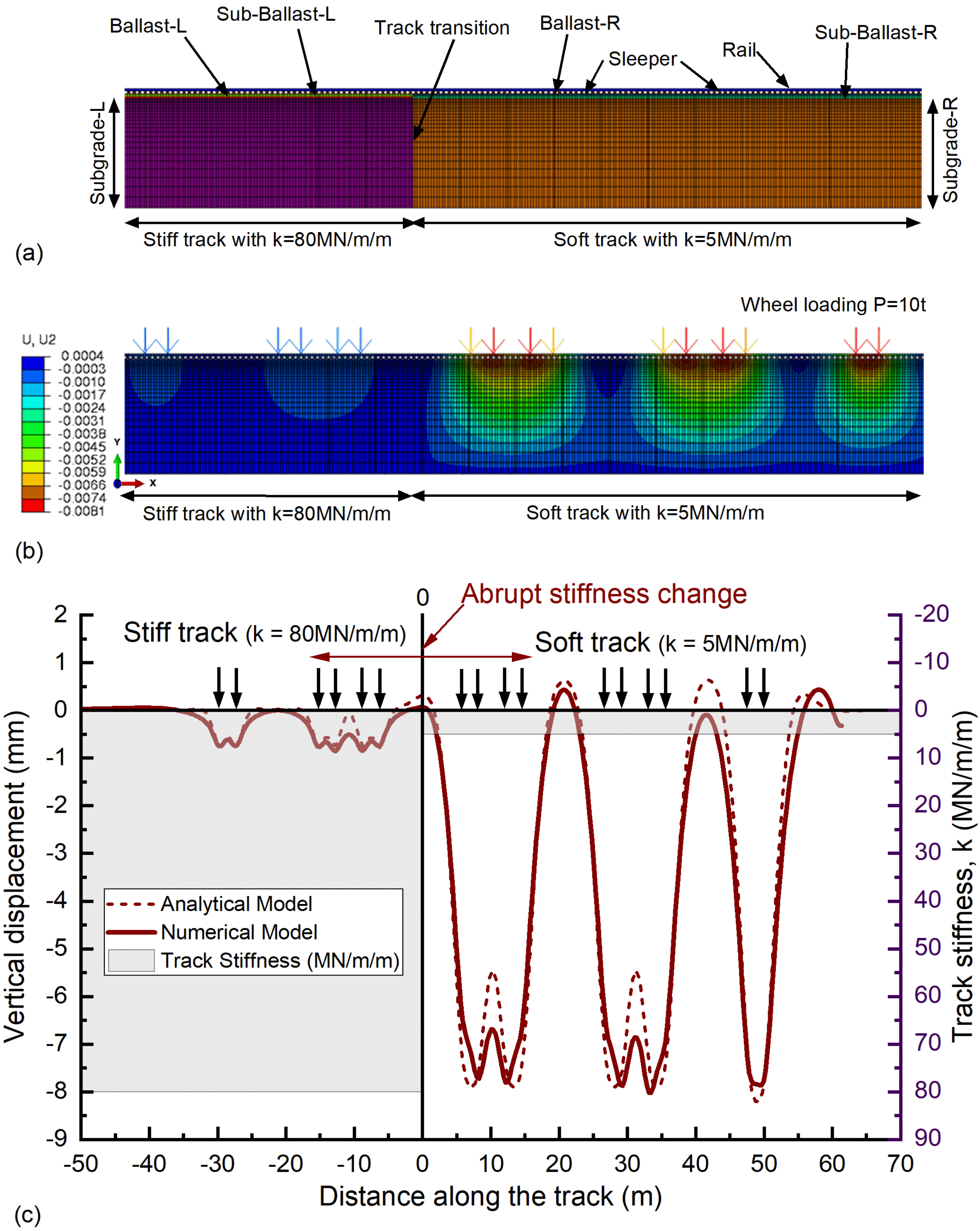

Fig. 14: (a) 2D FEM model for ballasted track transition for k-80MN/m/m and k=5MN/m/m track; (b) Deformation contours for 2D FEM layered model with abrupt stiffness variation at track transition under *P*=10 tonne; (c) Comparison of vertical displacements of rail track for one-step transition for analytical and numerical modelling.

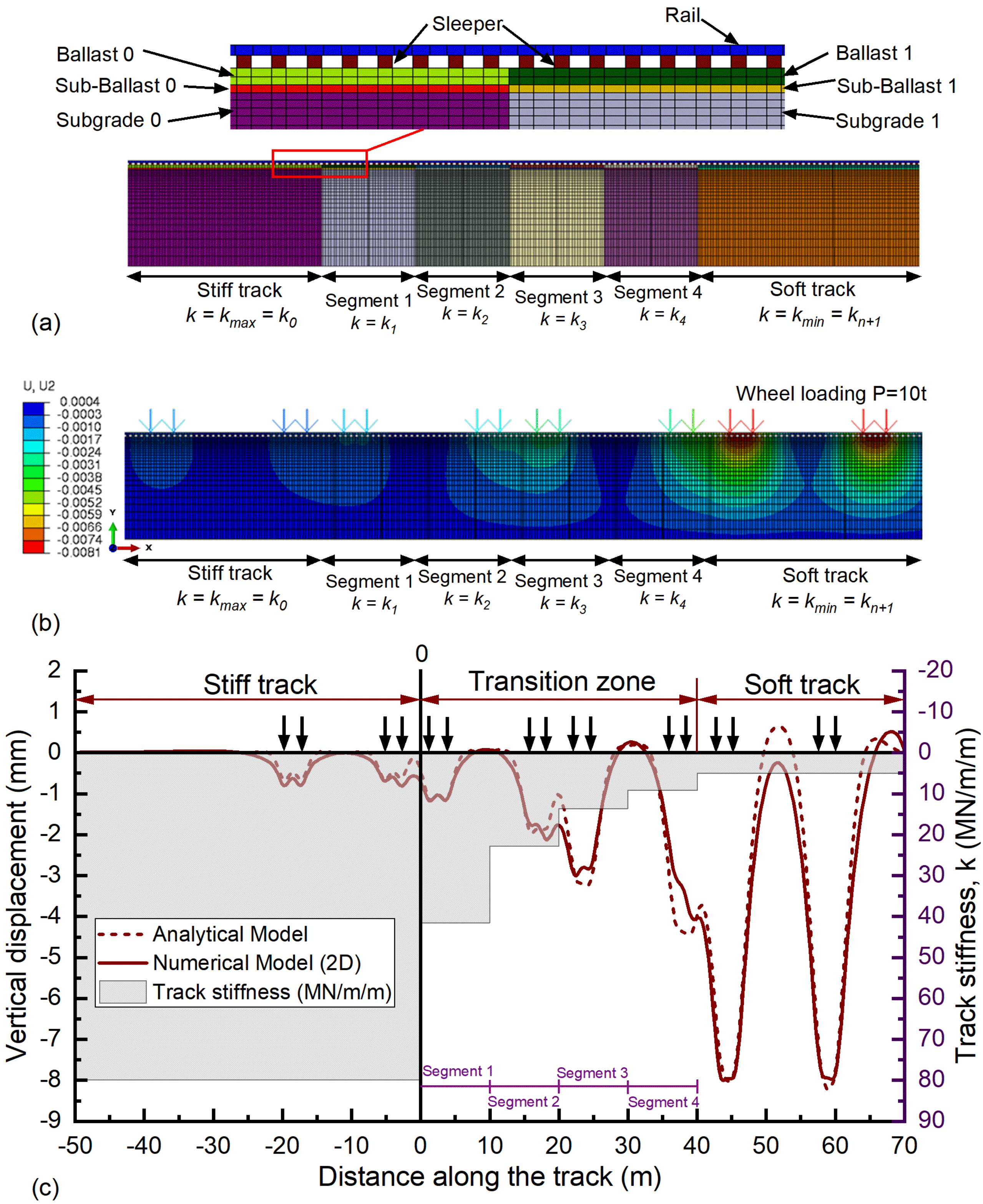

Fig. 15: (a) 2D FEM model for 5-steps ballasted track transition for k-80MN/m/m to k=5MN/m/m; (b) Deformation contours for 2D FEM layered model for 5-steps ballasted track transition for k-80MN/m/m to k=5MN/m/m; (c) Comparison of vertical displacements of rail track for 5-step transition for analytical and numerical modelling.

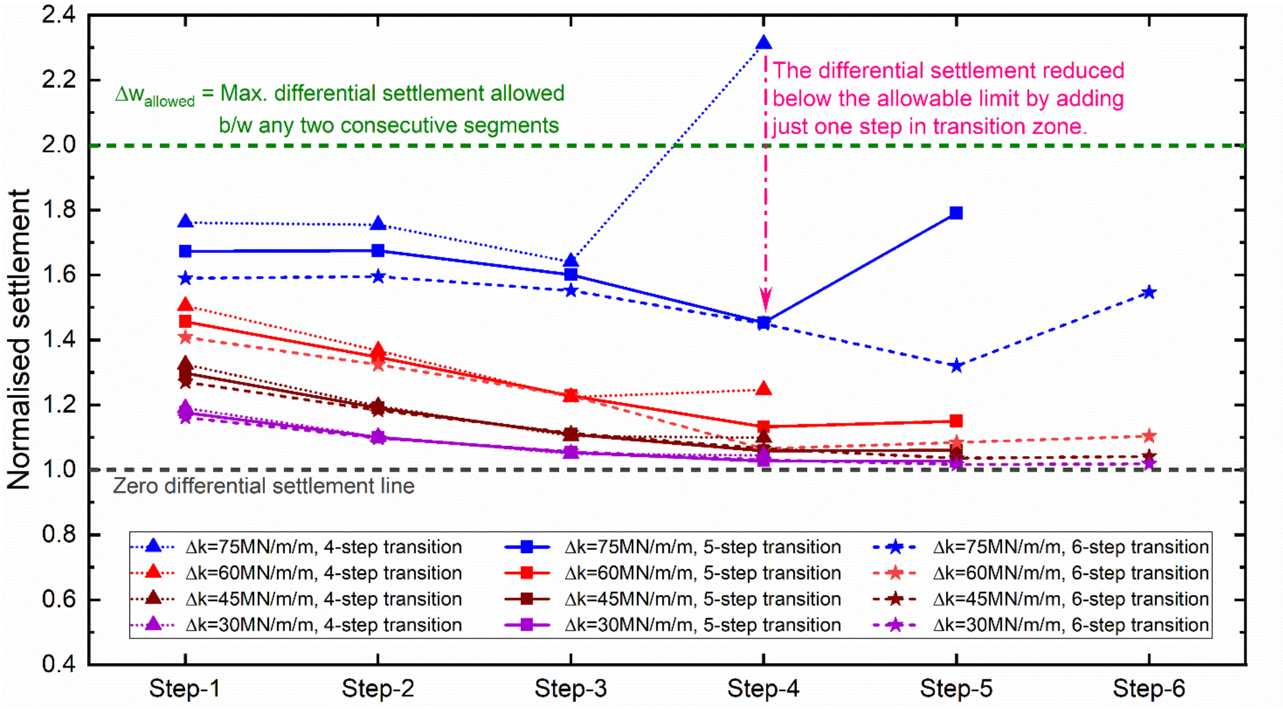

Fig. 16: Effect of stiffness variation (Δk) and number of transition steps on the design of transition zone

Table 1: Material properties used in ballasted track model

Track Components	**Value**
Rail	
Density (kg/m^3)	7850
Young's modulus (MPa)	210000
Poisson's ratio, ν	0.3
Sleeper	
Density (kg/m^3)	2500
Young's modulus (MPa)	30000
Poisson's ratio, ν	0.25
Ballast	
Density (kg/m^3)	1530
Young's modulus (MPa)	200
Poisson's ratio, ν	0.3
Rayleigh Damping Coefficient, α (1/s)	6.14
Rayleigh Damping Coefficient, β (s)	0.000195
Thickness (m)	0.3
Sub-ballast	
Density (kg/m^3)	1800
Young's modulus (MPa)	110
Poisson's ratio, ν	0.3
Rayleigh Damping Coefficient, α (1/s)	4.8
Rayleigh Damping Coefficient, β (s)	0.000152
Thickness (m)	0.15
Subgrade	
Density (kg/m^3)	1730
Young's modulus (MPa)	50
Poisson's ratio	0.4
Rayleigh Damping Coefficient, α (1/s)	4.8
Rayleigh Damping Coefficient, β (s)	0.000152
Thickness (m)	5

Table 2: Material properties for equivalent track stiffnesses

k (MN/m/m)	E_b (MPa)	E_c (MPa)	E_s (MPa)
5	200	110	8.5
9.2	200	150	15.7
10	200	150	17.2
13.6	200	150	23.6
20	250	150	35
22.8	250	150	40.5
40	250	175	75
41.5	250	175	80
80	300	175	175

Where, k is track equivalent stiffness, and E_b, E_c, and E_s is modulus of elasticity of ballast, sub-ballast and subgrade, respectively